Research Paper

THEMED ISSUE: Geologic Evolution of the Alaska Range and Environs

GEOSPHERE

GEOSPHERE, v. 15

https://doi.org/10.1130/GES01673.1

13 figures; 2 tables; 1 set of supplemental files

CORRESPONDENCE: jbenowitz@alaska.edu

CITATION: Benowitz, J.A., Davis, K., and Roeske, S., 2019, A river runs through it both ways across time: $^{40}Ar/^{39}Ar$ detrital and bedrock muscovite geochronology constraints on the Neogene paleodrainage history of the Nenana River system, Alaska Range: Geosphere, v. 15, https://doi.org/10.1130/GES01673.1.

Science Editor: Raymond M. Russo
Guest Associate Editor: James V. Jones III

Received 25 January 2018
Revision received 20 October 2018
Accepted 13 February 2019

A river runs through it both ways across time: $^{40}Ar/^{39}Ar$ detrital and bedrock muscovite geochronology constraints on the Neogene paleodrainage history of the Nenana River system, Alaska Range

Jeff A. Benowitz[1], Kailyn Davis[1], and Sarah Roeske[2]

[1]Geophysical Institute and Geochronology Laboratory, University of Alaska–Fairbanks, Fairbanks, Alaska 99775, USA
[2]Earth and Planetary Sciences Department, University of California–Davis, Davis, California 95616, USA

ABSTRACT

The Alaska Range, the topographic signature of the Denali fault, has an unusual physiography, with the Nenana River sourced from the south side of the divide and traversing along the range front some distance before heading north across the mountain range. Previous researchers suggested that a change from south-flowing to north-flowing drainage occurred at ca. 6 Ma, or early-middle Miocene, during initial phases of Alaska Range uplift. We applied $^{40}Ar/^{39}Ar$ dating of detrital micas from modern river sediment (proxy for basinwide source) and strata of the Neogene Tanana Basin (sink for the paleo–Nenana River), located along the northern front of the Alaska Range, to further investigate this hypothesis. In addition, we acquired $^{40}Ar/^{39}Ar$ muscovite ages from bedrock for additional source constraints and compared our results to regional geochronology data sets and geological mapping. During the earliest Miocene, the paleo–Nenana River likely flowed south. By the early Miocene, the paleo–Nenana River flowed to the north. During the middle Miocene, drainage reorganization continued, suggesting a variable history of rock uplift in the Alaska Range. By the late Miocene, sediment recycling occurred as the southern extent of the Tanana Basin was uplifted and eroded. The modern Nenana River near Cantwell has a muscovite age signature different than the Tanana Basin strata, implying continued drainage reorganization after the deposition of the Pliocene Nenana Gravel. In summary, the Nenana River drainage changed direction to north-flowing by ca. 18 Ma, driven by tectonism. Drainage reorganization continues today, demonstrating that strike-slip fault transpressive orogens can have complex paleodrainage histories.

INTRODUCTION

There have been numerous detrital geochronology studies examining drainage reorganization due to tectonism, with a focus on drainage changes linked to flat-slab subduction (e.g., Western Interior United States; Sharman et al., 2017) and continent-continent collision (e.g., Tibet; van Hoang et al., 2009). The application of detrital geochronology to investigate drainage reorganization of transpressive orogens along continental strike-slip faults has received less attention. Given that transpressive orogens are associated with complex topographic development histories (e.g., Spotila et al., 2007), and strike-slip fault–related orogenesis can lead to drainage reversals along incised canyons (Brocard et al., 2011), more case studies documenting the drainage evolution and potential river reversals linked to these dynamic mountain ranges are warranted.

The Alaska Range, located along the strike-slip Denali fault, has an unusual physiography, with two north-flowing river systems, the Nenana and Delta Rivers. These anomalous rivers are currently sourced from the south side of the topographic divide, indicating a potentially complex drainage reorganization history along a transpressive orogen (Fig. 1). These rivers traverse along the range front some distance before heading north and cutting through the mountain range (Fig. 2). Drainage reorganization of the Nenana River system, in particular, has long been linked to the timing of the development of the Alaska Range (Moffit, 1915; Wahrhaftig et al., 1969; Ridgway et al., 1999, 2007; Thoms, 2000; Brennan and Ridgway, 2015; Finzel et al., 2015, 2016).

Researchers have argued that there was a change from a generally south-flowing to north-flowing Nenana River at ca. 6 Ma, corresponding with the assumed initial uplift of the Alaska Range based on paleoflow data and clast composition (Wahrhaftig et al., 1969; Ridgway et al., 1999). Based on a more modern detrital zircon U-Pb geochronology study, Brennan and Ridgway (2015) inferred significant drainage reorganization was occurring much earlier, by the early-middle Miocene, but their source-to-sink detrital zircon U-Pb geochronology correlation was potentially nonunique. An early-middle Miocene timing of drainage reorganization is also ~10 to ~15 m.y. after the extensively documented initiation of Oligocene to present uplift of the Alaska Range, calling into question their conclusion (Benowitz et al., 2011, 2012a, 2014; Lease et al., 2016).

We built on Brennan and Ridgway's (2015) approach of using detrital zircon U-Pb geochronology to study the Nenana River drainage history by applying $^{40}Ar/^{39}Ar$ dating to detrital muscovite from strata of the Neogene Tanana Basin (sink for the paleo-Nenana River), located along the northern front of the Alaska Range (Figs. 1 and 3), and to detrital muscovite from modern river sediment (proxy for basinwide source; Fig. 1). In addition, we applied $^{40}Ar/^{39}Ar$ dating to

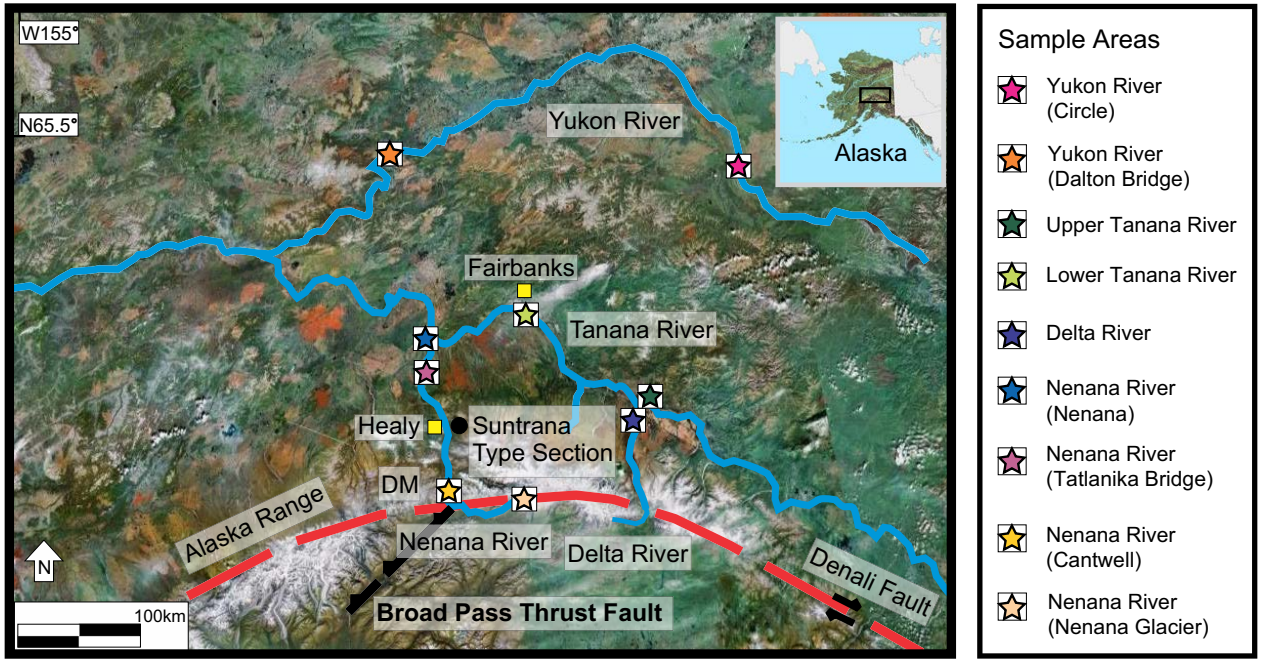

Figure 1. Regional map with study area and modern river sample locations annotated. Upper-right inset map shows satellite image location of Figure 1. We sampled the uplifted Tanana Basin at the Suntrana type section located near Healy, Alaska. Double Mountain (DM) is the location of Cantwell Basin strata detrital sample.

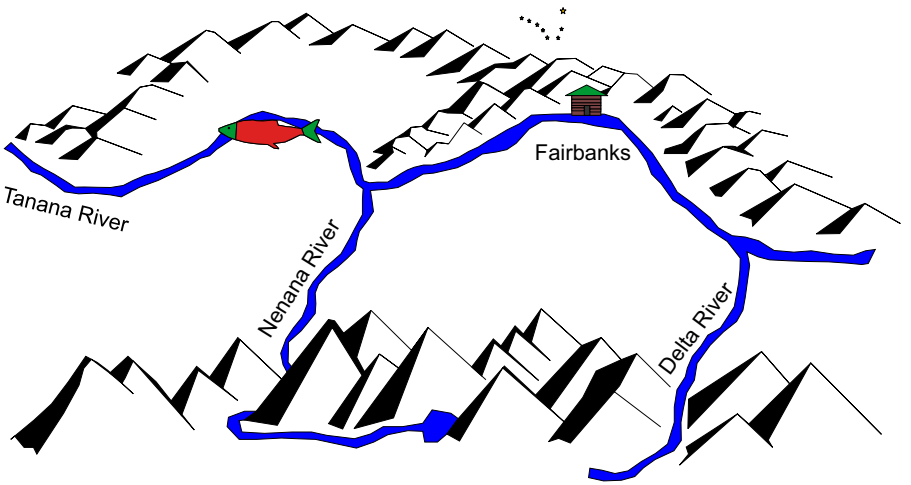

Figure 2. Artistic rendering of the Nenana and Delta Rivers starting south of the Alaska Range and flowing along the range front before turning north and passing through the Alaska Range.

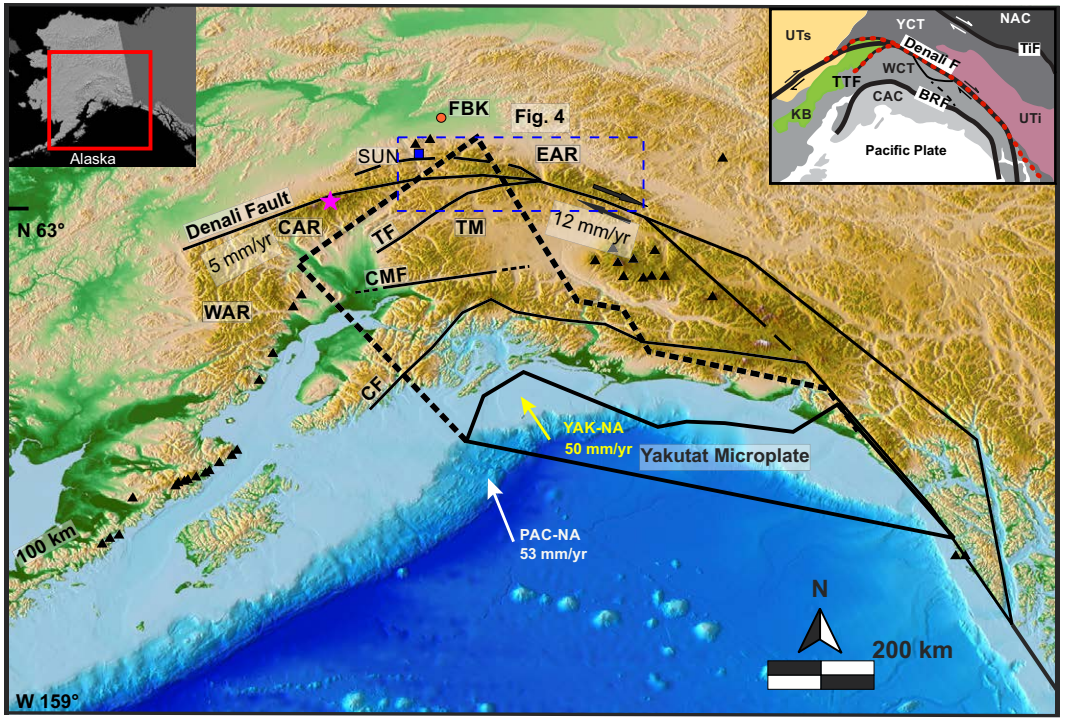

Figure 3. Digital elevation model (DEM) and simplified modern Yakutat flat-slab tectonic setting of southern Alaska. Upper-left inset map shows Figure 3 DEM location. Upper-right inset map shows major accreted terranes: YCT—Yukon-Tanana composite terrane, WCT—Wrangellia composite terrane, CAC—Chugach accretionary complex, TiF—Tintina fault, UTi—undifferentiated terranes and igneous rocks, UTs—unidentified terranes and sedimentary rocks, KB—Kahiltna Basin, TTF—Talkeetna fault, BRF—Border Ranges fault, NAC—North American craton, red dotted line—Mesozoic suture zone between continental and oceanic terranes. Main map: WAR—western Alaska Range, CAR—central Alaska Range, EAR—eastern Alaska Range, TM—Talkeetna Mountains, TF—Talkeetna fault, FBK—Fairbanks, CMF—Castle Mountain fault, CF—Contact fault, SUN—Suntrana type section (blue square), black triangles—modern volcanoes. Blue dashed rectangle—area on Figure 4. YAK-NA—Yakutat–North American plates; PAC-NA—Pacific–North American plates. Subducted Yakutat slab geometry is from Eberhart-Phillips et al. (2006). Slip rates are from Haeussler et al. (2017a). Figure is modified from Fitzgerald et al. (2014).

muscovite from select bedrock samples for additional source constraints and compared our results to regional geochronology data sets and geological mapping (Figs. 4 and 5). Our results indicate an earlier (ca. 18 Ma) and overall more prolonged history of Nenana River drainage reorganization than previously captured, but these results still support the general conclusions of Brennan and Ridgway (2015). This interpretation aligns well with published evidence of a complex temporal-spatial history of Oligocene to present uplift for the Alaska Range and further demonstrates the utility of combining modern river sediment detrital geochronology with dating of ancient strata and regional bedrock samples.

GEOLOGICAL BACKGROUND

Alaska Range Suture Zone, the Denali Fault, and the Alaska Range

The Mesozoic to Cenozoic Alaska Range suture zone is the tectonostratigraphic boundary between the Precambrian–Paleozoic Yukon-Tanana composite terrane of Laurentian affinity to the north and the accreted, primarily Mesozoic, oceanic rocks of the Wrangellia composite terrane of southern Alaska to the south (Figs. 3 and 6; Trop and Ridgway, 2007). These terranes are intruded and overlain by Devonian to Cenozoic igneous intrusive and volcanic rocks (Fig. 5; e.g., Wilson et al., 2015). The Alaska Range suture zone itself consists of the Kahiltna Basin, which is composed primarily of Late Jurassic to Late Cretaceous marine sedimentary strata (Ridgway et al., 2002), and the Late Cretaceous to Eocene terrestrial Cantwell Basin (Fig. 6; e.g., Tomsich et al., 2014; Salazar-Jaramillo et al., 2016). The Alaska Range suture zone is intruded and overlain by Mesozoic and Cenozoic igneous intrusive and volcanic rocks (Fig. 5) (e.g., Wilson et al., 2015). More recent work has led to the conclusion that these "composite" terranes and Kahiltna nomenclatures are an oversimplification of regions with very complex geologic histories (Hults et al., 2013; Dusel-Bacon et al., 2017; Dumoulin et al., 2018a, 2018b). For the goals of this paper, these vestigial terms are used because they clearly convey and delineate the geologic history of sediment sources north, south, and within the Alaska Range, and they are sufficiently different to reconstruct sediment source histories for the Nenana River system.

The Denali fault traverses the Alaska Range suture zone and has been an active strike-slip fault since at least ca. 65 Ma (e.g., Benowitz et al., 2014). Ancient and modern horizontal slip rates decrease to the west from ~12 mm/yr

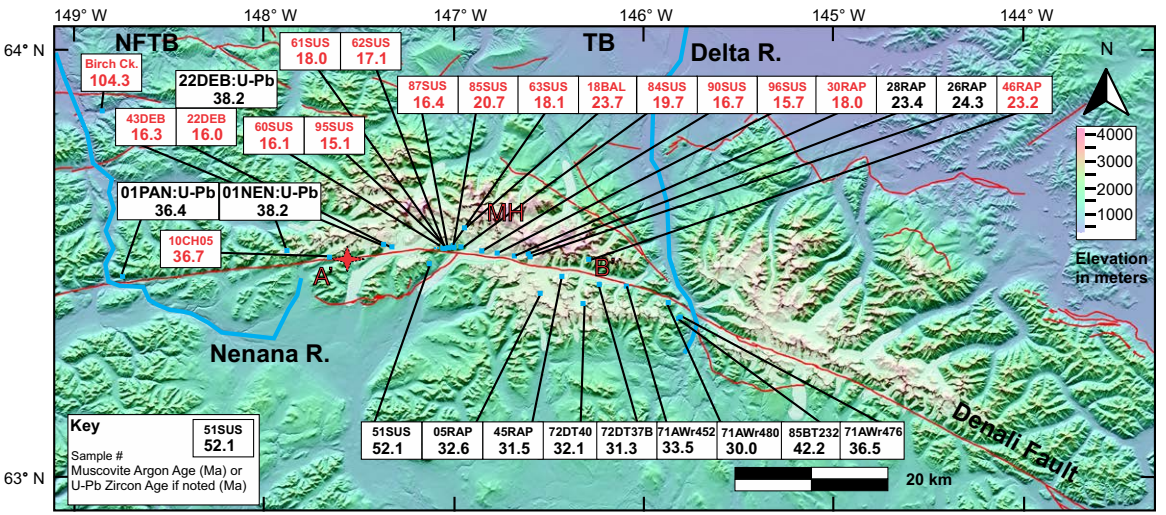

Figure 4. Digital elevation model of the high peak region of the eastern Alaska Range with sample locations and integrated $^{40}Ar/^{39}Ar$ muscovite ages from new (red, Ma) and published (black, Ma) bedrock samples. Red star is the location of the Nenana River headwaters ca. 37 Ma bedrock muscovite. See Table 1 for references. MH—Mount Hayes, TB—Tanana Basin, NFTB—Northern Foothills thrust belt. Sampling transect A′ to B′ is shown on Figure 11.

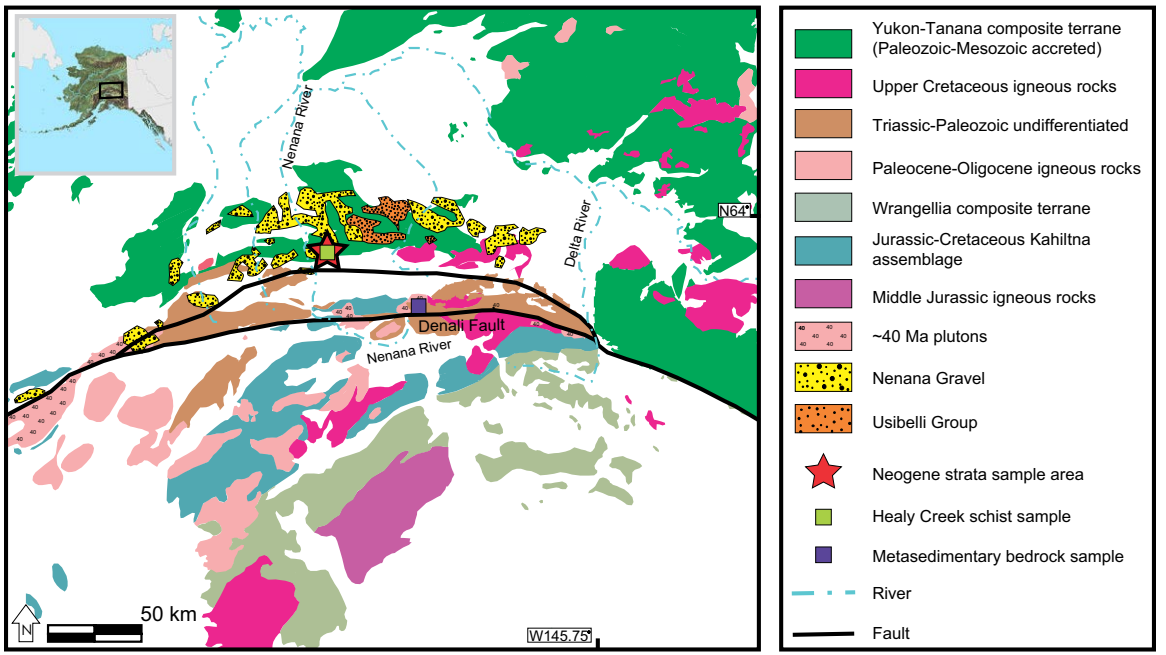

Figure 5. Regional geological map demonstrating across-strike variation of the Denali fault lithological units. Upper-right inset map shows Figure 5 geological map location. Triassic-aged rocks are present in the Alaska Range suture zone and Broad Pass. There are 153–201 Ma–aged rocks south of the Alaska Range suture zone within the Wrangellia composite terrane. The 120–153 Ma $^{40}Ar/^{39}Ar$ muscovite sources lie north of the Alaska Range suture zone in the Yukon-Tanana Highlands. There are known plutons within the Alaska Range suture zone that have the distinct emplacement age of ca. 40 Ma. Map is modified from Trop and Ridgway (2007).

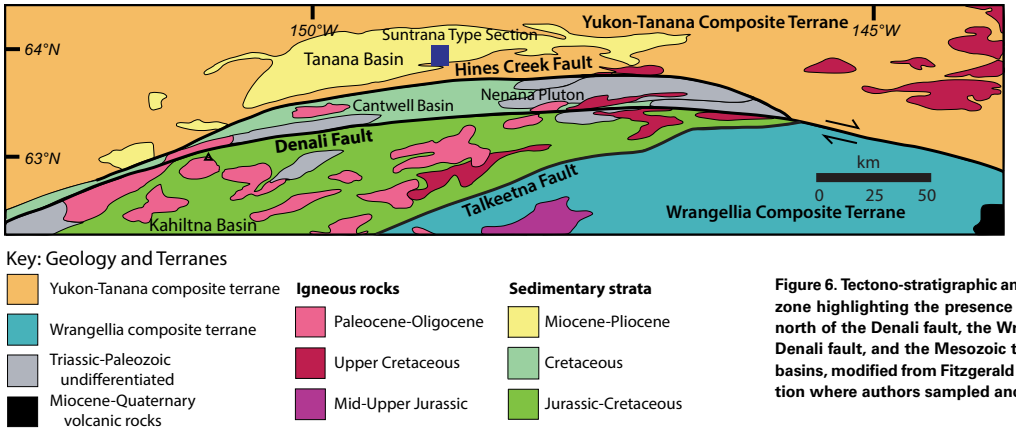

Figure 6. Tectono-stratigraphic and terrane map of the Alaska Range suture zone highlighting the presence of the Yukon-Tanana composite terrane north of the Denali fault, the Wrangellia composite terrane south of the Denali fault, and the Mesozoic to Cretaceous Alaska Range suture zone basins, modified from Fitzgerald et al. (2014). Blue square represents location where authors sampled ancient strata of the Tanana Basin.

to ~5 mm/yr (Benowitz et al., 2012b; Haeussler et al., 2017a), with slip taken up on contractional structures on both sides of the Denali fault (Riccio et al., 2014; Bemis et al., 2015; Waldien et al., 2015; Burkett et al., 2016), supporting evidence of a highly transpressive fault system (Fig. 3). Cenozoic magmatism was also associated with the trace of this major structure, with the last major period of plutonism at ca. 40 Ma (e.g., Wilson et al., 2015).

Thermochronology research has constrained the initial timing of uplift of the topographically high modern Alaska Range to ca. 30 to 25 Ma (Benowitz et al., 2014; Riccio et al., 2014; Burkett et al., 2016; Lease et al., 2016). These thermochronology studies and the aforementioned structural studies outline a history of asymmetrical uplift and unroofing of the Alaska Range through time and space along the Denali fault system. The way in which the complex topographic development history of the Alaska Range affected the paleodrainage history of the Nenana River system is the focus of this study.

Tanana Basin

The ancient and still-active Tanana Basin lies north of the Alaska Range, where the southern portion of the basin has been incorporated into the uplifted Alaska Range as the mountain range has encroached northward with time (Ridgway et al., 2007; Bemis and Wallace, 2007; Bemis et al., 2012, 2015). Approximately 2000 m of Neogene strata are exposed at the Suntrana type section located near Healy, Alaska (Fig. 1). These strata were deposited on the muscovite-rich Birch Creek schist basement rock of the Yukon-Tanana terrane (Fig. 6). The Tanana Basin strata are divided into the Miocene Usibelli Group and the Pliocene Nenana Gravel (Fig. 7; Leopold and Liu, 1994). At the type section, the Usibelli Group is ~800 m thick and is divided into five formations based on facies analysis (Wahrhaftig, 1987; Ridgway et al., 2007). These formations are the Healy Creek (earliest Miocene), Sanctuary (earliest Miocene), Suntrana (early-middle Miocene), Lignite Creek (late Miocene), and the Grubstake (latest Miocene) Formations, after Brennan and Ridgway (2015). The ~1200 m Pliocene Nenana Gravel unit conformably overlies the Grubstake Formation at the type section location (Wahrhaftig, 1987).

Paleodrainage History of the Nenana River System

Previous researchers have proposed three different interpretations of the paleodrainage history of the Nenana River. (1) Based on clast composition and paleoflow indicators, Wahrhaftig et al. (1969) and Ridgway et al. (1999) inferred that the Nenana River reversed direction from dominantly south-flowing to north-flowing shortly after the deposition of the Grubstake ash at ca. 6 Ma, based on $^{40}Ar/^{39}Ar$ analysis by Triplehorn et al. (2000). (2) Brennan and Ridgway (2015) conducted detrital zircon U-Pb geochronology analysis of six samples from the Suntrana type section and inferred a change in dominant paleoflow direction from south-directed to north-directed flow by the time of deposition of the middle Miocene (ca. 15 Ma) upper Suntrana Formation. (3) Based primarily on observations of past glacial distributions and topography, Moffit (1915) proposed a rerouting of the Nenana River due to inferred configurations of glaciers during the waning phase of the last glaciation.

PALEODRAINAGE RECONSTRUCTION TECHNIQUES

A diverse set of tools and techniques has been applied to modern rivers and ancient strata to identify tectonically driven drainage reorganization. Sedimentology features can provide information on paleoflow direction (Smith, 1972).

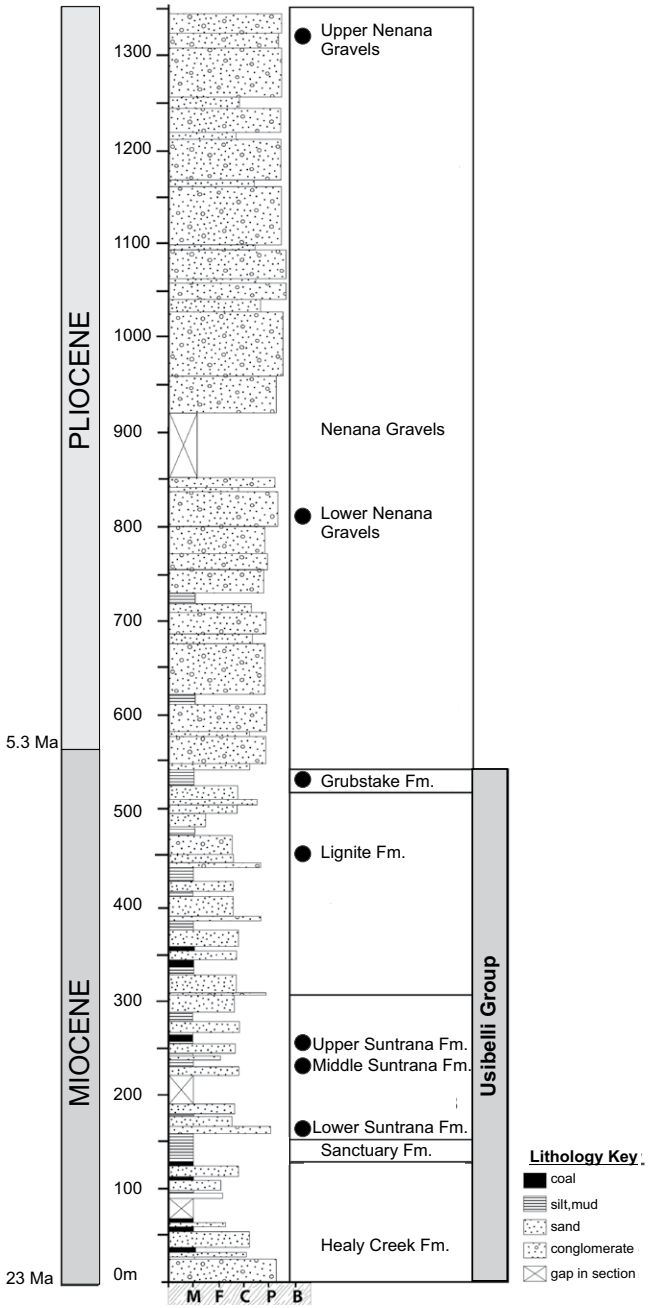

Figure 7. Measured stratigraphic section of the Usibelli Group and Nenana Gravel at the Suntrana type section. Formation names, stratigraphic ages, and approximate detrital muscovite sample stratigraphic positions are shown. Black circles indicate sample locations for detrital muscovite samples. Grain-size abbreviations: M—clay and silt; F—fine sand; C—coarse sand; P—pebble; B—boulder. Figure is modified from Brennan and Ridgway (2015).

Remote sensing has been applied to delineate potential paleodrainage systems (Wiedmer et al., 2010), as has analysis of variations in genetic diversity (Zhang and Sun, 2011). Arguably, the most commonly applied tool to study paleodrainage source-to-sink linkages is high-throughput detrital mineral geochronology (e.g., Cawood et al., 2012; Chirouze et al., 2013; Blum and Pecha, 2014).

Reconstruction of paleodrainage reorganization from detrital mineral age signatures is complicated due to the potential removal of source material through unroofing. Long-distance (>100 km) tectonic translation of basins away from source areas can also complicate interpretation. More foundational, the requirement for nonunique sources is not always met and can lead to equivocal findings. These concerns can be mitigated by: (1) applying provenance source-to-sink geochronology to minerals and radiometric systems that represent different mineral densities, potentially unique lithologies, and crustal depths, such as U-Pb geochronology on zircons and $^{40}Ar/^{39}Ar$ geochronology on muscovite grains, and (2) complementary dating of source areas through geochronology analysis of bedrock samples and modern river sediment.

Detrital $^{40}Ar/^{39}Ar$ muscovite geochronology can capture different source lithologies than detrital U-Pb zircon geochronology due to the factors listed below. Fertility or mineral abundance has a strong effect on detrital geochronology source populations. Detrital U-Pb zircon geochronology is well suited for capturing the age signatures of regional plutonism (e.g., Cawood et al., 2012); detrital $^{40}Ar/^{39}Ar$ muscovite geochronology is well suited for capturing the age signatures of regional metamorphism (e.g., Hodges et al., 2005). The density of minerals also has a strong effect on detrital geochronology source populations. Zircon is a dense mineral (specific gravity: 4.9 g/cc), and so source area populations can be fractionated during transport and deposition as they move primarily as bed load (van Hoang et al., 2010; Lawrence et al., 2011). Muscovite is a lighter mineral (specific gravity: 2.8 g/cc), but muscovite age populations still can be fractionated during transport and deposition (e.g., Garzanti et al., 2008). Muscovite is more likely to be transported as suspended sediment compared to zircon, due to the lower density of muscovite and basal cleavage properties.

By combining detrital $^{40}Ar/^{39}Ar$ muscovite geochronology (this study) with the interpretations based on detrital U-Pb zircon geochronology techniques (Brennan and Ridgway, 2015), an increased understanding can be obtained of drainage system reorganization in response to the development of a transpressional orogen. In the framework of previous U-Pb zircon work on the paleodrainage history of the Alaska Range (Brennan and Ridgway, 2015), we applied $^{40}Ar/^{39}Ar$ geochronology to detrital muscovite from Neogene strata of the Tanana Basin at the Suntrana type section, to modern river sediment from rivers south and north of the Suntrana type section, and to select bedrock samples to better evaluate the paleodrainage history of the Nenana River.

POTENTIAL MUSCOVITE SOURCES FOR THE NENANA RIVER SYSTEM

To the south of the Alaska Range suture zone, the Jurassic Talkeetna arc plutons (153–201 Ma) are a dominant lithology with abundant muscovite (Fig. 5; Hacker et al., 2011; Terhune et al., 2017). To the north of the Alaska Range suture zone, the basement schist, which has predominantly Cretaceous metamorphic ages, is the identifying lithology of the Yukon-Tanana composite terrane (Fig. 6; Hansen et al., 1991; Dusel-Bacon et al., 1996). The Yukon River drainage encompasses terranes with Jurassic $^{40}Ar/^{39}Ar$ muscovite age signatures (Gehrels et al., 2009; Staples et al., 2016; Jones et al., 2017), but by the Eocene, it was likely separated from the Tanana River drainage by the high topography of the Yukon-Tanana Highlands (Dusel-Bacon et al., 2016). The Mesozoic Kahiltna and early Cenozoic Cantwell Basin units contain sparse large-grained (>250 µm) primary metamorphic and detrital muscovite, and so they cannot be fully discounted as potential sources for recycled muscovite for the Neogene strata of the Tanana Basin.

Numerous ca. 40 Ma plutons are mapped on the north side of the Denali fault zone in proximity to the Suntrana type section, but they are not present regionally to the north or south (Figs. 5 and 6; Roeske et al., 2012; e.g., Wilson et al., 2015). These plutons provide a potential unique source for both detrital zircon and muscovite grains for the Tanana Basin, but zircons of this age have not been documented in the ancient strata of the Tanana Basin (Brennan and Ridgway, 2015). The lack of zircons from these plutons is likely not related to a mineral fertility concern, because of their felsic lithology. Additional ca. 40 Ma plutons south of the Denali fault, located >100 km east of the Suntrana type section, contain abundant muscovite. However, these plutons were likely translated ~250 km into place during the Neogene, thus discounting them as a source for muscovite in the Neogene Tanana Basin located north of the Denali fault (Fig. 5; Nokleberg et al., 1985, 1992; Benowitz et al., 2012b).

To the north, strata of the Oligocene to Quaternary Tanana Basin overlie the Yukon-Tanana composite terrane (Ridgway et al., 2007). The well-dated strata of the Tanana Basin generally contain abundant and large-grained (>250 µm) muscovite, providing a potential geochronology fingerprinting tool with which to reconstruct the Oligocene to Quaternary paleodrainage reorganization history of the Nenana River system. The Oligocene to Quaternary strata of the Tanana Basin are also a potential source of progressively recycled muscovite, as the basin has been inverted variably through time and space (Ridgway et al., 2007).

METHODS

Tanana Basin Sampling Strategy

We collected muscovite-rich sandstone, mudstone, and sand samples from the Usibelli Group and Nenana Gravel at the Suntrana type section (Healy Creek site) using the formation descriptions and published photos to select sample locations within the section (Fig. 7; e.g., Ridgway et al., 2007; Brennan and Ridgway, 2015). Given that the change from north-derived to south-derived sediment provenance was documented between the lowermost strata of the Suntrana Formation (ca. 20 Ma) and the uppermost strata of the Suntrana Formation (ca. 15 Ma) by Brennan and Ridgway (2015), we collected three spaced samples from this formation to better delineate when the change in sediment provenance occurred. A total of ~20 L of generally muscovite-rich material was collected from the lowermost strata of the Suntrana Formation (sandstone collected), middle strata of the Suntrana Formation (mudstone collected), upper strata of the Suntrana Formation (sandstone collected), and the Grubstake Formation (mudstone collected). For the thicker Nenana Gravel unit, we collected a lower sand sample and upper sand sample within the section. The lower Nenana Gravel sample had limited muscovite. All other ancient strata samples had abundant muscovite grains of desired size (~500 to ~250 µm).

Modern River Sampling Strategy

We collected ~20 L of generally muscovite-rich modern river sediment from rivers north and south of the Alaska Range suture zone (Fig. 1). All samples contained substantial quantities of muscovite, except for the two samples from the upper stretches of Nenana River, as noted below. The west-flowing upper (community of Delta site) and lower (community of Fairbanks site) Tanana River samples primarily capture sediment sourced from the Yukon-Tanana Highlands watershed. The north-flowing Delta River sample potentially captures sediment sourced from the Yukon-Tanana composite terrane and the Alaska Range suture zone. The west-flowing Yukon River samples (town site of Circle City and the Dalton Highway Bridge) capture local watershed sediment sources and potentially sediment sourced from Canada. The south-flowing Nenana Glacier outlet sample (headwaters of the Nenana River) captures sediment sourced from the Alaska Range suture zone. This river sample had very limited muscovite. The west-flowing Nenana River sample (Cantwell Bridge) captures sediment primarily sourced from the Alaska Range suture zone in the Nenana Glacier area. This river sample also had very limited muscovite. The north-flowing Nenana River samples at the Tatlanika Bridge site and at the townsite of Nenana potentially capture sediment derived from the Yukon-Tanana composite terrane, the Alaska Range suture zone, and potentially recycled sediment from the Tanana Basin.

Bedrock Sampling Strategy

Bedrock samples (~4 kg per sample site) were collected to better delineate potential sources for the muscovite of the Tanana Basin and the exhumation history of the Alaska Range. We sampled the muscovite-rich Birch Creek schist basement rock at the Suntrana type section at the base of the Healy Creek

Formation to evaluate a local bedrock source for muscovite in the Tanana Basin strata. In total, 16 muscovite-bearing deformed igneous and metasedimentary samples from the Alaska Range suture zone north of the Denali fault were collected. We divided these samples into granitoid or metasediment. Many of these granitoid samples are orthogneiss or mylonites; hence, the muscovite closure temperature for these samples may be below ~400 °C (e.g., Martin et al., 2015). We complemented our bedrock data with existing bedrock geochronology data sets (Hansen et al., 1991; Nokleberg et al., 1992; Gehrels et al., 2009; Greene et al., 2010; Perry et al., 2010; Hacker et al., 2011; Benowitz et al., 2011, 2014) and geological maps (Dusel-Bacon et al., 1996; Wilson et al., 2015). Additionally, one sample was collected from the ca. 70 Ma strata (Tomsich et al., 2014) of the Cantwell Formation (Fig. 1).

$^{40}Ar/^{39}Ar$ Muscovite Geochronology Methods

We applied $^{40}Ar/^{39}Ar$ single-grain fusion detrital geochronology (Hodges et al., 2005; Broussard et al., 2018) to the modern river sediment samples and the Tanana Basin strata samples. We applied $^{40}Ar/^{39}Ar$ muscovite geochronology incremental step-heating analysis (McDougall and Harrison, 1999) to pure muscovite separates (1000–250 µm grain size) from the 16 bedrock samples from the Alaska Range suture zone and the single Birch Creek schist basement sample at the Suntrana type section.

We separated out ~50–200 grains of 500–250-µm-sized muscovite from each modern river sediment sample and from each sandstone/mudstone sample from the Suntrana type section. In addition to standard mineral separation techniques (floating muscovite in water, paper shaking, Frantz magnetic separation), we occasionally used a stainless-steel rolling pin to "roll" samples in order to break up quartz flakes, which were then removed with repeated sieving. Only two detrital muscovite grains were separated from the Cantwell Basin sample, and so those results are not very robust, but since this data set is likely the first from detrital muscovite from this Alaska Range suture zone Cretaceous basin, we present the data in the Supplemental Material[1]. The $^{40}Ar/^{39}Ar$ age determinations were performed by J. Benowitz at the Geochronology Facility at the University of Alaska–Fairbanks. Refer to Supplemental Text for detailed $^{40}Ar/^{39}Ar$ geochronology methods.

$^{40}Ar/^{39}Ar$ GEOCHRONOLOGY RESULTS

Bedrock $^{40}Ar/^{39}Ar$ Geochronology

The $^{40}Ar/^{39}Ar$ analysis of the 16 bedrock samples provided robust results with plateau ages and integrated ages generally overlapping within error. Preferred age determinations and isotopic data are provided in Table 1 and Tables S1 and S2 (see footnote 1). Example age spectra are presented in Figure 8, with all age spectra, Ca/K, and Cl/K data presented in Figure S1. Isochron age determinations were not always possible due to the generally homogeneous nature of the gas release for many samples. When an isochron age determination was possible, the age and isotopic information are presented in Table 1 and Figure S1. The isochron regressions to $^{40}Ar/^{36}Ar$ indicate no prevailing evidence of excess ^{40}Ar. We plotted integrated ages on Figure 4 because the integrated age of an incremental step-heating analysis is the equivalent of a single fusion age, which is the method we used on the detrital samples from the ancient Suntrana type section strata and modern river sediment muscovite. Details of representative Alaska Range bedrock samples are outlined below.

A muscovite separate from the basement Birch Creek schist was analyzed, and the integrated age (104.3 ± 1.1 Ma) and the plateau age (104.8 ± 1.5 Ma) were within error (Table 1; Figs. 4 and 8; Fig. S1 [see footnote 1]). A muscovite separate from metasediment sample 10CH05B, collected at the headwaters of the Nenana River, was analyzed, and the integrated age (36.7 ± 0.3 Ma) and the plateau age (36.4 ± 0.2 Ma) were within error (Table 1; Figs. 4 and 8; Fig. S2). A muscovite separate from 18BAL, a granitoid sample along the north side of the Denali fault, was analyzed, and the integrated age (23.7 ± 0.3 Ma), plateau age (23.7 ± 0.2 Ma), and isochron age (23.5 ± 0.2 Ma) were all within error (Table 1; Figs. 4 and 8; Fig. S1). A muscovite separate from 45RAP, an orthogneiss sample along the south side of the Denali fault, was analyzed, and the integrated age (31.5 ± 0.1 Ma) and the plateau age (31.6 ± 0.1 Ma) were within error (Table 1; Figs. 4 and 8; Fig. S1).

Overall Detrital Muscovite $^{40}Ar/^{39}Ar$ Geochronology

Not all of the detrital single-grain fusion technique muscovite grains that were analyzed produced useable results. We applied a 20% error filter to eliminate muscovite grains with (1) low precision, (2) high atmospheric ^{40}Ar content, which is associated with alteration and leads to high % error, and (3) detrital grains that may not have been muscovite grains (>1 Ca/K), which can also lead to high % error. Each sample yielded between two (Cantwell Basin strata) and 92 single-grain muscovite ages. For the middle Suntrana Formation, we ran a second aliquot based on the documented first presence of unique Alaska Range–sourced ca. 37 Ma muscovite grains in the Tanana Basin strata and thus dated 163 middle Suntrana Formation muscovite grains total. River locations are presented in Table S3 (see footnote 1). Modern river sediment and ancient strata muscovite single-grain fusion age determinations, probability density plots, and isotopic data are provided in Tables 2, S4–S6, Figures 9, S2, and S3.

We binned each muscovite grain age into subdivisions of 0–50 Ma (Alaska Range), 50–120 Ma (source area that is nonunique), 120–153 Ma (Yukon-Tanana Highlands), 153–201 Ma (Wrangellia composite terrane age and Stikine terrane potential source), and Triassic period (201–250 Ma) based on regional geochronology data sets and mapping, our new bedrock data set, and the modern river sediment age signatures. Four grains (251, 265, 269, and 550 Ma) from the combined analysis of all the strata samples fell outside of these

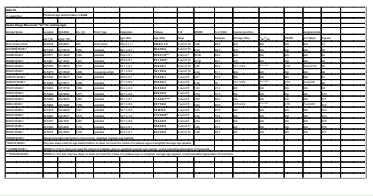

[1]Supplemental Material. Isotopic data tables and figures and sample locations. Please visit https://doi.org/10.1130/GES01673.S1 or access the full-text article on www.gsapubs.org to view the Supplemental Material.

TABLE 1. COMPILATION OF NEW AND PUBLISHED BEDROCK $^{40}Ar/^{39}Ar$ AND K-Ar MUSCOVITE COOLING AGES AND PUBLISHED U-Pb ZIRCON AGES FROM THE GREATER NENANA PLUTON

Sample name	Lat (°N)	Long (°W)	North or south of Denali fault	Rock type	Integrated age (Ma)	Error age ± (Ma)
New results: Alaska Range muscovite $^{40}Ar/^{39}Ar$ cooling ages						
Birch Creek schist	63.8516	148.8407	North	Muscovite schist	104.3	1.1
10CH05B MU#L1	63.5156	147.6574	North	Metasediment	36.7	0.3
43DEB MU#L1	63.5371	147.3649	North	Granitoid	16.6	0.1
22DEB MU#L1	63.5391	147.3237	North	Granitoid	16.0	0.1
60SUS MU#L1	63.5339	147.0872	North	Granitoid	16.1	0.1
95SUS MU#L1	63.5279	147.0548	North	Muscovite schist	15.1	0.2
61BSUS MU#L1	63.5336	147.0517	North	Granitoid	18.0	0.1
62ASUS MU#L1	63.5336	147.0517	North	Granitoid	17.1	0.2
87SUS MU#L1	63.5284	147.0154	North	Granitoid	16.4	0.2
85SUS MU#L1	63.5349	146.9954	North	Granitoid	20.7	0.6
63SUS MU#L1	63.5388	146.9919	North	Granitoid	18.1	0.1
18BAL MU#L1	63.5808	146.9405	North	Granitoid	23.7	0.2
84SUS MU#L1	63.5318	146.9549	North	Granitoid	19.7	0.5
90SUS MU#L1	63.5205	146.8477	North	Granitoid	16.7	1.0
96SUS MU#L1	63.5167	146.7641	North	Granitoid	15.7	0.6
30RAP MU#L1	63.5160	146.6847	North	Granitoid	18.0	0.1
46RAP MU#L1	63.5075	146.3052	North	Granitoid	23.2	0.1
Published results: Alaska Range muscovite $^{40}Ar/^{39}Ar$ cooling ages						
26RAP MU#L1§	63.5193	146.601	North	Granitoid	24.3	0.1
28RAP MU#L1§	63.5148	146.6136	North	Granitoid	23.4	0.1
51SUS MU#L1#	63.4983	147.1329	South	Granitoid	52.1	0.3
05RAP MU#L1**	63.4337	146.5411	South	Granitoid	32.6	0.3
45RAP MU #L1**	63.4723	146.431	South	Granitoid	31.5	0.1
72DT40 MU††	63.4050	146.3250	South	Granitoid	32.1	0.9
72DT37B MU†† (K-Ar)	63.4517	146.2383	South	Granitoid	31.3	0.9
71AWr452†† (K-Ar)	63.4100	145.8750	South	Granitoid	33.5	1.0
71AWr480†† (K-Ar)	63.4517	146.0750	South	Granitoid	30.0	0.9
85BT232†† (K-Ar)	63.3667	145.7933	South	Granitoid	42.2	1.0
71AWr476†† (K-Ar)	63.3700	145.8183	South	Granitoid	36.5	1.1
Published results: Alaska Range U-Pb zircon ICP-MS ages						
01PAN†	63.4672	148.7354	North	Granitoid	36.4	0.5
01NEN††	63.5308	147.8830	North	Granitoid	38.2	0.5
22DEB††	63.5391	147.3237	North	Granitoid	38.2	0.9

Note: Latitude and longitude are given in World Geodetic System 1984 (WGS84) coordinates. ICP-MS—inductively coupled plasma–mass spectrometry. Samples are located on Figure 4.
†Perry et al. (2010).
§Benowitz et al. (2014).
#Riccio et al. (2014).
**Benowitz et al. (2011).
††Nokleberg et al. (1992).

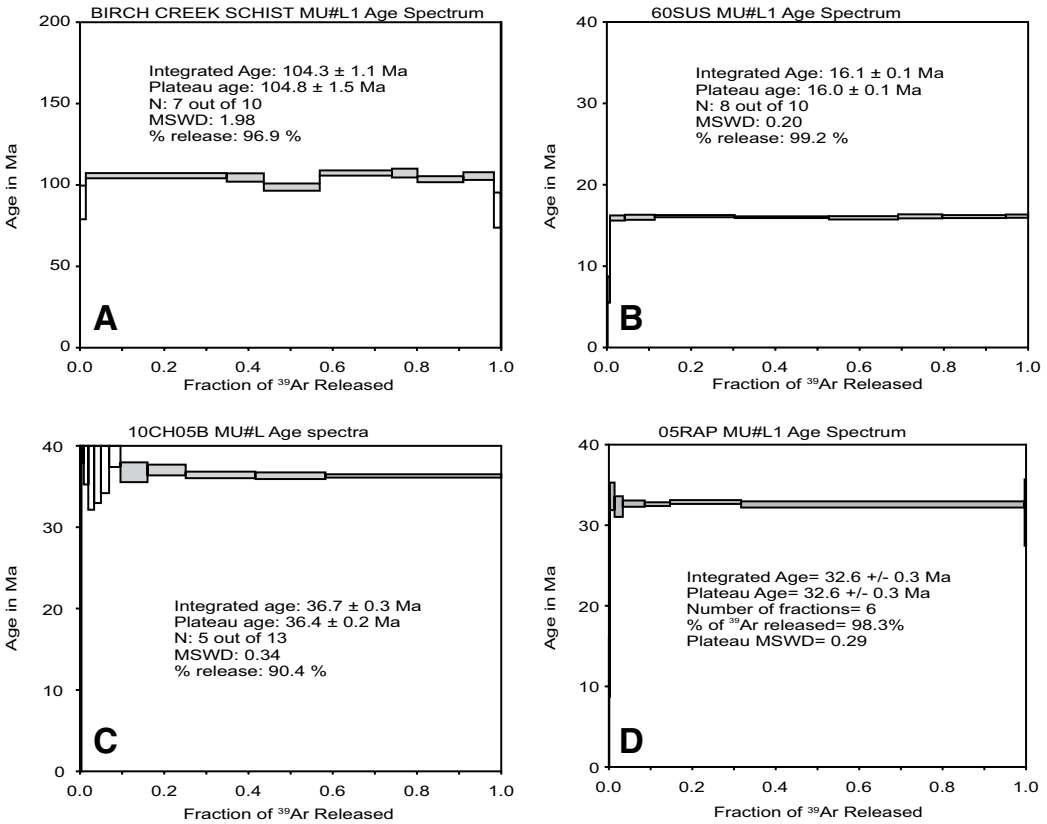

Figure 8. Example age spectra from newly dated $^{40}Ar/^{39}Ar$ muscovite from bedrock. Sample locations are on Figure 4. MSWD—mean square of weighted deviates.

age bins and were not assigned a source or used in population comparisons because of their limited presence.

Modern River Sediment Detrital Muscovite $^{40}Ar/^{39}Ar$ Geochronology

We used the modern river sediment detrital muscovite signatures to tune both our age bins and source signatures. Muscovite-dominant unique age populations from the Delta River, upper Tanana River, and lower Tanana River sites all exhibit primarily a Yukon-Tanana Highlands source (120–153 Ma), with limited Wrangellia composite terrane and Stikine terrane (153–201 Ma) input (Table 2; Figs. 1, 9A, 9B, and 9C). The Nenana Glacier outlet and Nenana River at the Cantwell Bridge sites both are dominated by an intra–Alaska Range source (0–50 Ma; Table 2; Figs. 1, 9D, and 9E). We recovered very few muscovite grains from the Nenana Glacier sample (10 successfully dated), reflecting the low fertility of muscovite in this predominantly granodiorite lithology watershed. There were no unique dominant age populations of muscovite from the Nenana River sample at the Tatlanika Bridge nor the sample site from the town of Nenana (Table 2; Figs. 1, 9F, and 9G). The dominant unique age populations of muscovite from the Yukon River samples collected at the Circle City townsite and the Dalton Highway Bridge were derived from either the Wrangellia composite terrane and/or Stikine terrane (153–201 Ma) and Yukon-Tanana Highlands sources (120–153 Ma; Table 2; Figs. 1, 9H, and 9I).

Tanana Basin Strata Detrital Muscovite $^{40}Ar/^{39}Ar$ Geochronology

The detrital muscovite age populations of the Tanana Basin strata (Table 2; Fig. 9) generally matched all the components present in the modern river

TABLE 2. COMPILATION OF DETRITAL MUSCOVITE AGE DATA FOR THE MODERN RIVER SAMPLES AND THE NEOGENE TANANA BASIN STRATA

River modern sediments	0–50 Ma	50–120 Ma	120–153 Ma	153–201 Ma	201–250 Ma	= Total
Yukon: Circle	% = 0	% = 46	% = 15	% = 36	% = 3	= 67
	= 0	= 31	= 10	= 24	= 2	
Yukon: Dalton Bridge	% = 0	% = 73	% = 9	% = 17	% = 1	= 80
	= 0	= 58	= 7	= 14	= 1	
Delta: Delta	% = 1	% = 61	% = 37	% = 1	% = 0	= 95
	= 1	= 58	= 35	=1	= 0	
Upper Tanana: Delta	% = 0	% = 47	% = 51	% = 1	% = 1	= 92
	= 0	= 43	= 47	= 1	= 1	
Lower Tanana: Fairbanks	% = 0	% = 60	% = 39	% = 1	% = 0	= 89
	= 0	= 53	= 35	= 1	= 0	
Nenana Glacier	% = 100	% = 0	% = 0	% = 0	% = 0	= 10
	= 10	= 0	= 0	= 0	= 0	
Nenana: Cantwell	% = 87	% = 13	% = 0	% = 0	% = 0	= 30
	= 26	= 4	= 0	= 0	= 0	
Nenana: Tatlanika	% = 0	% = 88	% = 6	% = 5	% = 1	= 81
	= 0	= 71	= 5	= 4	=1	
Nenana: Nenana	% = 0	% = 94	% = 3	% = 3	% = 0	= 31
	= 0	= 29	= 1	= 1	= 0	

Formation	0–50 Ma	50–120 Ma	120–153 Ma	153–201 Ma	201–250 Ma	= Total
Upper Nenana Gravels (Pliocene)	% = 0	% = 70	% = 17	% = 11	% = 2	= 46
	= 0	= 32	= 8	= 05	= 1	
Lower Nenana Gravels (Pliocene)	% = 0	% = 53	% = 28	% = 16	% = 3	= 36
	= 0	= 19	= 10	= 6	= 1	
Grubstake (latest Miocene)	% = 2	% = 40	% = 27	% = 26	% = 5	= 101
	= 2	= 41	= 27	= 26	= 5	
Lignite (late Miocene)	% = 4	% = 48	% = 14	% = 29	% = 5	= 120
	= 5	= 57	= 17	= 35	= 6	
Upper Suntrana (middle Miocene)	% = 1	% = 50	% = 13	% = 22	% = 14	= 74
	= 1	= 37	= 10	= 16	= 10	
Middle Suntrana (early Miocene)	% = 4	% = 51	% = 12	% = 31	% = 2	= 163
	= 7	= 84	= 19	= 50	= 3	
Lower Suntrana (early Miocene)	% = 0	% = 74	% = 21	% = 3	% = 2	= 66
	= 0	= 49	= 14	= 2	= 1	

Notes: Age bins were determined by regional detrital muscovite age data, bedrock maps, and geochronology data sets (see text). The lower Suntrana Formation cells colored blue have strong north-of-the-Alaska-Range $^{40}Ar/^{39}Ar$ muscovite age affinities. The middle Suntrana Formation cells colored yellow have strong south-of-the-Alaska-Range and intra–Alaska Range $^{40}Ar/^{39}Ar$ muscovite age affinities.

sediment samples (Table 2; Fig. 10), but the individual age percentages varied greatly between the individual formations (Figs. S2 and S3 [see footnote 1]). We did not have any detrital muscovite data from rivers draining Wrangellia composite terrane watersheds. During the deposition of the earliest Miocene lower Suntrana Formation, the dominant unique age population of muscovite showed a Yukon-Tanana Highlands source age signature (21%; 120–153 Ma), with limited Wrangellia composite terrane and Stikine terrane–aged muscovite present (3%; 153–201 Ma; Table 2; Figs. 7 and 10A). During the deposition of the early Miocene middle Suntrana Formation, the dominant unique age population of the muscovite showed a Wrangellia composite terrane and Stikine terrane source age signature (31%; 153–201 Ma) and an additional population unique to the Alaska Range (4%; 0–50 Ma) with limited Yukon-Tanana Highlands source–aged muscovite (12%; 120–153 Ma; Table 2; Figs. 7 and 10B).

The middle Miocene upper Suntrana Formation has a large (compared to all the other strata samples) contribution of Triassic-aged muscovite grains (14%; 201–250 Ma) and a single grain (1%) from an age population unique to

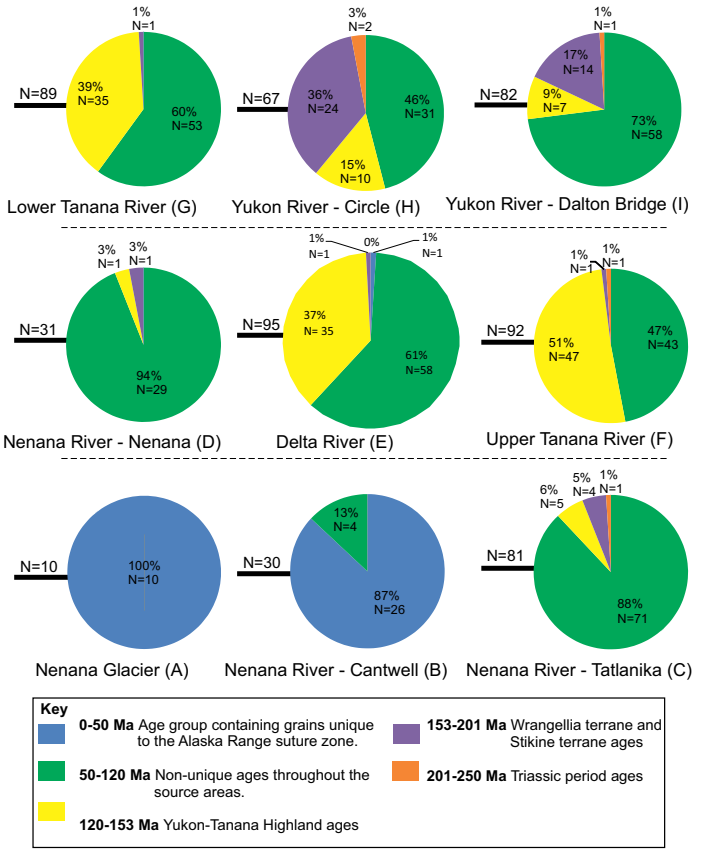

Figure 9. Pie chart plots of the detrital $^{40}Ar/^{39}Ar$ muscovite modern river age data set demonstrating variations in watershed source ages.

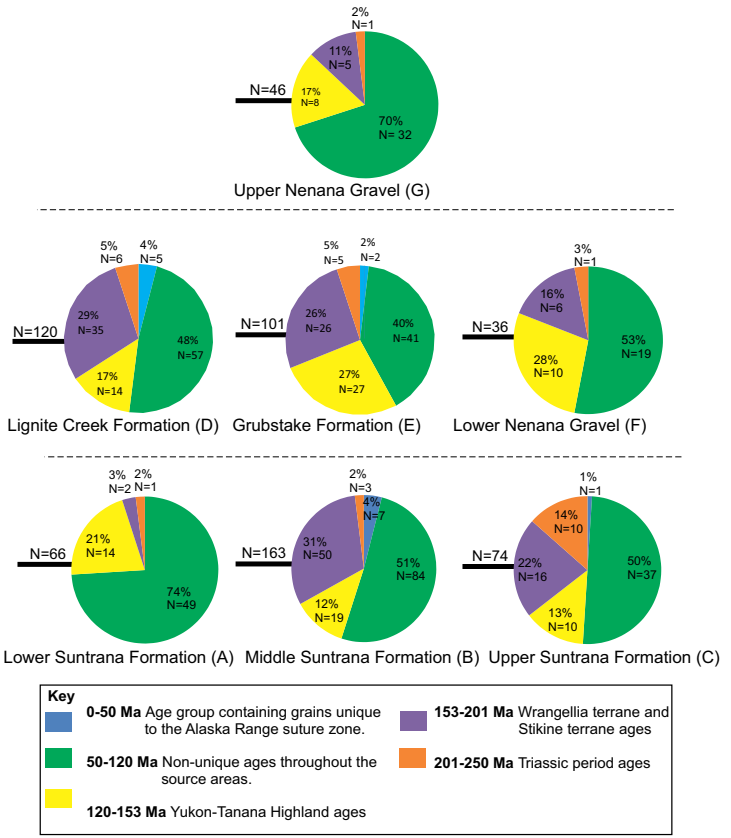

Figure 10. Pie chart plots of the detrital $^{40}Ar/^{39}Ar$ muscovite Tanana Basin strata age data set demonstrating variations in components through time.

the Alaska Range (0–50 Ma; Table 2; Figs. 1 and 10C). The Yukon-Tanana Highlands source age signature is still limited (13%; 120–153 Ma). The presence of Wrangellia composite terrane and Stikine terrane–aged muscovite is still higher (22%; 153–201 Ma) compared to the older lower Suntrana Formation (3%; 153–201 Ma). During the deposition of the late Miocene Lignite Creek Formation, the dominant unique age population of muscovite has a Wrangellia composite terrane and Stikine terrane source age signature (31%; 153–201 Ma) and an additional population unique to the Alaska Range (4%; 0–50 Ma), with limited Yukon-Tanana Highlands source–aged muscovite (12%; 120–153 Ma; Table 2; Figs. 1 and 10D).

During the deposition of the latest Miocene Grubstake Formation, there are unique age populations of muscovite with Wrangellia composite terrane and Stikine terrane source ages (26%; 153–201 Ma) and Yukon-Tanana Highlands source–aged muscovite (27%; 120–153 Ma), with an additional population unique to the Alaska Range (2%; 0–50 Ma; Table 2; Figs. 1 and 10E). We did not date >50 muscovite grains for the Nenana Gravel samples, and so our age populations may not be fully reflective of the age fractions present in these strata (Dodson et al., 1988; Vermeesch, 2004). However, the number of grains needed per sample is dependent on the source and sink detrital geochronology complexity (Vermeesch, 2004). Given both the limited number of muscovite age populations present in the modern river sediment and the ancient strata as a whole, dating 36 grains (lower Nenana Gravel sample) ensures a 95% certainty that no fraction greater than 14% was uncaptured from the muscovite detrital population present (Vermeesch, 2004). Dating 46 grains (upper Nenana

Gravel sample) ensures a 95% certainty that no fraction greater than 11% was uncaptured from the muscovite detrital population present. During deposition of the Pliocene lower Nenana Gravel unit, the dominant unique age populations of the muscovite are Yukon-Tanana Highlands source–aged muscovite (28%; 120–153 Ma) and Wrangellia composite terrane and Stikine terrane source ages (16%; 153–201 Ma; Table 2; Figs. 1 and 10F). During the deposition of the Pliocene to Quaternary upper Nenana Gravel unit, the dominant unique age populations of muscovite are Yukon-Tanana Highlands source–aged muscovite (17%; 120–153 Ma) and Wrangellia composite terrane and Stikine terrane source age signatures (11%; 153–201 Ma; Table 2; Figs. 1 and 10G).

Cantwell Basin Strata

The single sample from the ca. 70 Ma Cantwell Basin strata yielded two grains with ages of ca. 138 and ca. 135 Ma (Table S6 [see footnote 1]), similar to grain ages from the Yukon-Tanana Highlands. Given the size (<~250 µm) and limited presence of muscovite in the Cantwell Basin strata observed, it is hard to interpret this limited data set. We present it as possible supporting evidence that flow direction was from the north during the Late Cretaceous (Ridgway et al., 1997) and suggest that further detrital muscovite work on the Mesozoic basins of the Alaska Range suture zone may provide fruitful results.

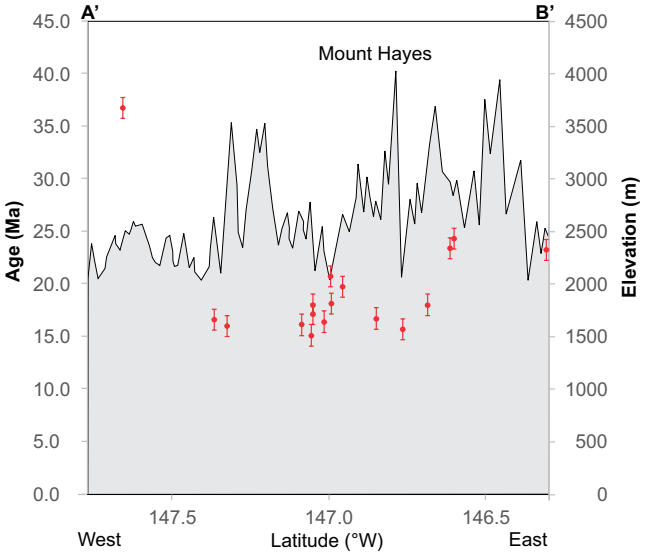

Figure 11. Muscovite $^{40}Ar/^{39}Ar$ ages for bedrock north of the Denali fault located within 5 km of the fault zone demonstrating west-to-east variations in muscovite ages. The variations in muscovite ages are indicative of asymmetrical exhumation patterns along the strike of the Denali fault. Topographic profile of the high ridgeline along the sampling transect is plotted. Sampling transect A' to B' is shown on Figure 4.

DISCUSSION

Alaska Range Bedrock Muscovite $^{40}Ar/^{39}Ar$ Geochronology

The $^{40}Ar/^{39}Ar$ muscovite age for the mica-rich Birch Creek schist underlying the Suntrana type section is ca. 105 Ma (Figs. 4 and 8). All the examined strata of the Tanana Basin have muscovite age populations overlapping this age. The age of the Birch Creek schist falls into the nonunique age bin of 50–120 Ma, which is present in all our modern river sediments, except the Nenana Glacier outlet sample. These results make it difficult to discern if local schist units outcropping as either topographic highs or the walls of river canyons were a contributing sediment source to the ancient Tanana Basin strata.

As previous researchers have noted, there is a distinct difference in eastern Alaska Range muscovite $^{40}Ar/^{39}Ar$ cooling ages across the Denali fault (Benowitz et al., 2011). Muscovite $^{40}Ar/^{39}Ar$ cooling ages to the south of the Denali fault are ca. 30 Ma to ca. 50 Ma. Muscovite $^{40}Ar/^{39}Ar$ cooling ages to the north of the Denali fault are ca. 15 Ma to ca. 30 Ma, with one metasedimentary bedrock sample north of the Denali fault having an age of ca. 37 Ma (Table 1; Figs. 4 and 11). We interpret this muscovite age to reflect formation, resetting, or recrystallization of mica during the emplacement of the ca. 40 Ma suite of plutons along the Nenana Glacier. Metamorphic and thermal aureoles of large plutons can be over ~2 km wide (Annen, 2017). The presence of these uniquely sourced muscovites in the Tanana Basin strata, where corresponding ca. 40 Ma zircons are not recorded (Brennan and Ridgway, 2015), can be explained by unroofing of the shallower metamorphic aureole of these plutons before the plutons themselves.

The break in muscovite $^{40}Ar/^{39}Ar$ cooling ages across the Denali fault reflects the documented history of deeper Neogene exhumation along the north side of the Denali fault in the Mount Hayes segment of the Alaska Range compared to the south side of the fault (Figs. 4 and 12; Benowitz et al., 2011, 2014). The population of muscovite cooling ages at ca. 25 Ma is in line with the initiation of flat-slab subduction of the Yakutat microplate at ca. 30 Ma (Brueseke et al., 2019), northwest convergence of southern Alaska across the Denali fault, and increased slip rates along the Denali fault since this time (Figs. 4 and 12; Benowitz et al., 2012b; Lease et al., 2016; Davis et al., 2017). An increase in Pacific plate–Alaska obliquity and convergence rate at ca. 25 Ma (Jicha et al., 2018) was also likely a factor driving increased rates of deformation along the Denali fault system. The east-to-west variation in $^{40}Ar/^{39}Ar$ muscovite cooling ages north of the Denali fault supports evidence of variable exhumation through time and space for the high peak region of the eastern Alaska Range (Benowitz et al., 2011, 2014). The muscovite $^{40}Ar/^{39}Ar$ cooling ages south of the Denali fault likely reflect the timing of regional pluton emplacement, metamorphism, and uplift (Fig. 4; e.g., Riccio et al., 2014).

Modern River Sediment Detrital Muscovite $^{40}Ar/^{39}Ar$ Geochronology Source Classification

The Nenana River at its headwaters (Nenana Glacier outlet sample) and at Cantwell (Table 2; Figs. 1 and 9) has clear intra–Alaska Range suture zone signatures. Downstream, this signal is drowned out by primary schist sources and possibly recycled Tanana Basin strata (Table 2; Figs. 1 and 9). The Delta River, upper Tanana River, and lower Tanana River samples have primarily Yukon-Tanana Highlands $^{40}Ar/^{39}Ar$ muscovite age signatures, which we refer to as north-sourced in the following discussion (Table 2; Figs. 1 and 9).

The Yukon River samples have dominantly Wrangellia and Stikine terrane $^{40}Ar/^{39}Ar$ muscovite age signatures (Table 2; Figs. 1 and 9). Logically, these 153–201 Ma–sourced muscovites did not come from south of or within the Alaska Range suture zone, but are more likely sourced from the Stikine terrane in Canada or local sources in the Yukon-Tanana composite terrane (Jones et al., 2017). Hence, 153–201 Ma $^{40}Ar/^{39}Ar$ muscovite ages are not in themselves unique to south or north of the Alaska Range suture zone, nor are the U-Pb zircon ages (Brennan and Ridgway, 2015). Changes in the proportion of Yukon-Tanana Highlands $^{40}Ar/^{39}Ar$ muscovite ages and the presence of $^{40}Ar/^{39}Ar$ muscovite ages unique to the Alaska Range suture zone are needed to discern if the 153–201 Ma $^{40}Ar/^{39}Ar$ muscovite ages are likely south and intra–Alaska Range suture zone–sourced or north-sourced.

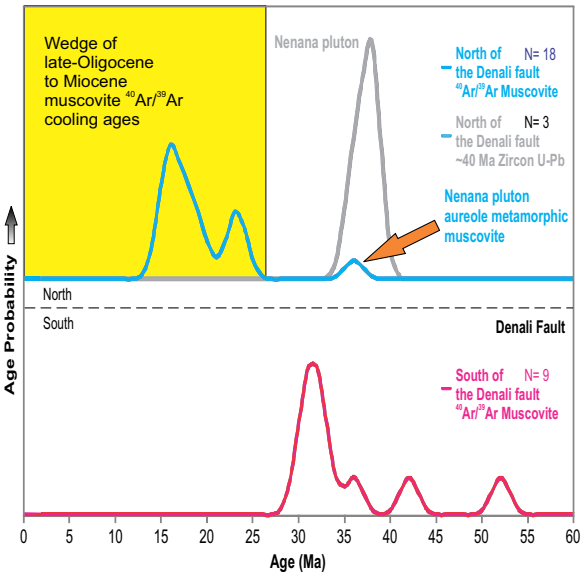

Figure 12. Bedrock $^{40}Ar/^{39}Ar$ muscovite ages north versus south of the Denali fault, demonstrating asymmetrical exhumation patterns across the strike of the Denali fault. U-Pb zircon ages for three ca. 40 Ma pluton samples from the greater Nenana pluton are shown in gray (Perry et al., 2010).

Nenana River Drainage Reconstruction

We did not sample the earliest Miocene Healy Creek Formation. Based on detrital U-Pb zircon geochronology and clast composition, Brennan and Ridgway (2015) concluded that the main source for sediment in the Tanana Basin during this time period was from the Yukon-Tanana composite terrane located to the north. This interpretation adds support to the Yukon-Tanana Highlands being a topographic high by this time period, if not earlier (Eocene; Dusel-Bacon et al., 2016).

Neither Brennan and Ridgway (2015) nor this study sampled the earliest Miocene Sanctuary Formation. Ridgway et al. (2007) interpreted the Sanctuary Formation as reflecting a regional early Miocene rapid subsidence event. Rapid subsidence is often driven by tectonic changes (Beaumont, 1981), and so the paleogeographic interpretation of Ridgway et al. (2007) is consistent with findings by other researchers (e.g., Lease et al., 2016) indicating that the Alaska Range was developing by early Miocene time.

During the deposition of the early Miocene lower Suntrana Formation, the paleo–Nenana River system likely derived sediment from north of the Alaska Range suture zone, based on the dominance of muscovite from the Yukon-Tanana Highlands to the north (21%; 120–153 Ma) and limited Wrangellia terrane–aged muscovite (3%; 153–201 Ma; Fig. 10A). This interpretation aligns well with the detrital U-Pb zircon geochronology and sedimentological conclusions of Brennan and Ridgway (2015), who stated that the main source for sediment for the Tanana Basin during this time period was from the north. The lack of potentially Stikine-aged muscovite (3%; 153–201 Ma) also adds support to the Yukon-Tanana Highlands being a topographic high by this time period, if not earlier (Eocene; Dusel-Bacon et al., 2016).

By the time of deposition of the early Miocene middle Suntrana Formation, sediment sources included significant mica from south of the Alaska Range suture zone and within the Alaska Range, based on: (1) the observed large increase in 153–201 Ma $^{40}Ar/^{39}Ar$ muscovite grains (3% to 31%) compared to the underlying lower Suntrana Formation, (2) a corresponding decrease in north-sourced Yukon-Tanana Highlands–affinity $^{40}Ar/^{39}Ar$ muscovite grains (21% to 12%) compared to the underlying lower Suntrana Formation, and (3) an additional population of ages unique to the Alaska Range suture zone (4%; 0–50 Ma; Table 2; Fig. 10B). Alternatively, the large increase in 153–201 Ma $^{40}Ar/^{39}Ar$ muscovite grains in the middle Suntrana Formation may have been derived from the Yukon River watershed to the north. However, this is unlikely due to (1) the documented high topography between the Yukon River and the Tanana River system (Dusel-Bacon et al., 2016), (2) the limited number of grains (<1%) in this age range present in the modern Tanana River samples (Table 2), (3) the decrease in Yukon-Tanana Highlands–affinity $^{40}Ar/^{39}Ar$ muscovite grains compared to the lower Suntrana Formation, and (4) the presence of grains that only have a known source from within the Alaska Range.

One factor of note, Brennan and Ridgway (2015) did not sample the middle Suntrana Formation, limiting comparisons between the detrital geochronology methods applied here. Ridgway et al. (2007) interpreted an increase in volcanic and plutonic/greenstone clasts in the Suntrana Formation compared to the Healy Creek Formation as reflecting a contribution of sediment from the south. Brennan and Ridgway (2015) documented a change in provenance between the lowermost Suntrana Formation and the upper Suntrana Formation, which supports our interpretation that by the time of middle Suntrana Formation deposition, there was a change in sediment source from north-dominated to south and intra–Alaska Range sourced.

The middle Miocene upper Suntrana Formation shows a continued dominant presence of 153–201 Ma $^{40}Ar/^{39}Ar$ muscovite grains compared to north-sourced $^{40}Ar/^{39}Ar$ muscovite grains (22% to 13%), with an additional limited population unique to the Alaska Range (1%; 0–50 Ma; Table 2; Fig. 10C). The middle Miocene upper Suntrana Formation also has a large contribution of Triassic $^{40}Ar/^{39}Ar$ muscovite grains (14%; 201–250 Ma) compared to the other strata samples analyzed. This indicates a likely variable history of rock uplift in the Alaska Range, which has also been documented through bedrock thermochronology studies (e.g., Benowitz et al., 2014; Lease et al., 2016; this study). This is also the stratum and time period in which Brennan and Ridgway (2017) observed a change in sediment provenance, supporting additional drainage reorganization at this time.

The late Miocene Lignite Formation has a continued dominant presence of 153–201 Ma $^{40}Ar/^{39}Ar$ muscovite grains compared to north-sourced $^{40}Ar/^{39}Ar$ muscovite grains (29% to 14%), with an additional population unique to the Alaska Range (4%; 0–50 Ma; Table 2; Fig. 10D). During this time period, Brennan and Ridgway (2015) inferred that the focus of exhumation in the Alaska Range varied and included sediment sourced from the exhuming Cantwell Basin (Figs. 5 and 6).

The latest Miocene Grubstake Formation has the reappearance of a high percentage of $^{40}Ar/^{39}Ar$ muscovite grains sourced from north of the Alaska Range (26%), with the addition of a contribution of grains sourced from south of the Alaska Range (27%) and a population unique to the Alaska Range (2%; 0–50 Ma; Table 2; Fig. 10E). We interpret this to indicate that by this time, the Healy Creek Formation strata located to the south and rich in clasts from Yukon-Tanana composite terrane–derived schist (Ridgway et al., 2007) were being exhumed and recycled, based on the increase of Yukon-Tanana Highlands $^{40}Ar/^{39}Ar$ muscovite grains in the Grubstake Formation strata. Lower Suntrana Formation strata to the south were also potentially being recycled by this time, based on our $^{40}Ar/^{39}Ar$ muscovite results, demonstrating that this stratum had a primarily north-derived muscovite age signature.

Brennan and Ridgway (2015) did not sample the Grubstake Formation, limiting comparisons between methods applied, but our interpretation of a latest Miocene inversion of the Tanana Basin to the south providing recycled sediment is consistent with theirs for the occurrence of recycling during deposition of the Pliocene Nenana Gravel unit. A clast petrology and provenance study of the Usibelli Group and Nenana Gravel also supports recycling of sedimentary basins to the south of this depositional zone during the latest Miocene to Pliocene, based on a dramatic increase in the presence of sandstone clasts in the Grubstake Formation compared to lower down in the section (Ridgway et al., 1999).

During the deposition of the Pliocene lower Nenana Gravel unit, the dominant age population is north-sourced compared to 153–201 Ma $^{40}Ar/^{39}Ar$ muscovite grains (28% to 16%). During the deposition of the Pliocene upper Nenana Gravel unit, the dominant age population is north-sourced compared to 153–201 Ma $^{40}Ar/^{39}Ar$ muscovite grains (17% to 11%). Both these Nenana Gravel samples produced limited $^{40}Ar/^{39}Ar$ muscovite ages, but the detrital U-Pb zircon study of Brennan and Ridgway (2015) provided addition support for our interpretation. Brennan and Ridgway (2015), as we do, inferred that this was a time of continued inversion and recycling of the Healy Creek and lower Suntrana Formation strata to the south.

The modern Nenana River near Cantwell has an 87% contribution of muscovite grains from the Alaska Range suture zone and no 153–201 Ma $^{40}Ar/^{39}Ar$ muscovite grains. The lack of Wrangell composite terrane–aged muscovite grains in the modern Nenana River implies that bedrock south of the Alaska Range is no longer a sediment source for the Tanana Basin. Based on this observation, we conclude that there was continued drainage reorganization after the deposition of the Nenana Gravel unit, likely driven by slip on the Broad Pass fault or other possible inferred thrusts similar to the Susitna thrust, which were active during the Quaternary (Fig. 1; Riccio et al., 2014; Haeussler et al., 2017b).

A compilation of apatite fission-track data from 17 igneous clasts collected from the Suntrana type section (Nenana Gravel unit) provides additional insight into the regional history of Alaska Range unroofing (Perry, 2014). Apatite fission-track data broadly represent the time a rock sample cooled through an ~100 °C isotherm, which is inferred to represent a depth of ~3 to ~5 km (e.g., Beamud et al., 2011). Nine of the 17 measured apatite fission-track Nenana Gravel clast ages are ca. 20 Ma, implying this was a period of regional unroofing upstream in the Alaska Range. These thermochronology timing constraints fit well with our interpretation that the upper Nenana River reversed direction by ca. 18 Ma due to tectonic activity in the Alaska Range. The overall apatite fission-track clast data set of Perry (2014) also indicates a complex regional unroofing history that aligns well with our interpretation, i.e., that the Alaska Range has experienced a prolonged and complex topographic development history.

An examination of the sediment provenance of Cenozoic strata from Cook Inlet (Fig. 13) provides an independent test of the interpretation that there was an Oligocene river system draining into Cook Inlet that originated north of the Alaska Range. Finzel et al. (2015) concluded, based on detrital U-Pb zircon provenance analysis, that there was an Oligocene regional drainage system with headwaters north of the Alaska Range. They inferred that sediment derived from the Yukon-Tanana Highlands was transported across the Alaska Range and deposited in Cook Inlet until the Miocene. Combined zircon U-Pb geochronology and fission-track double-dating of Cenozoic strata in Cook Inlet

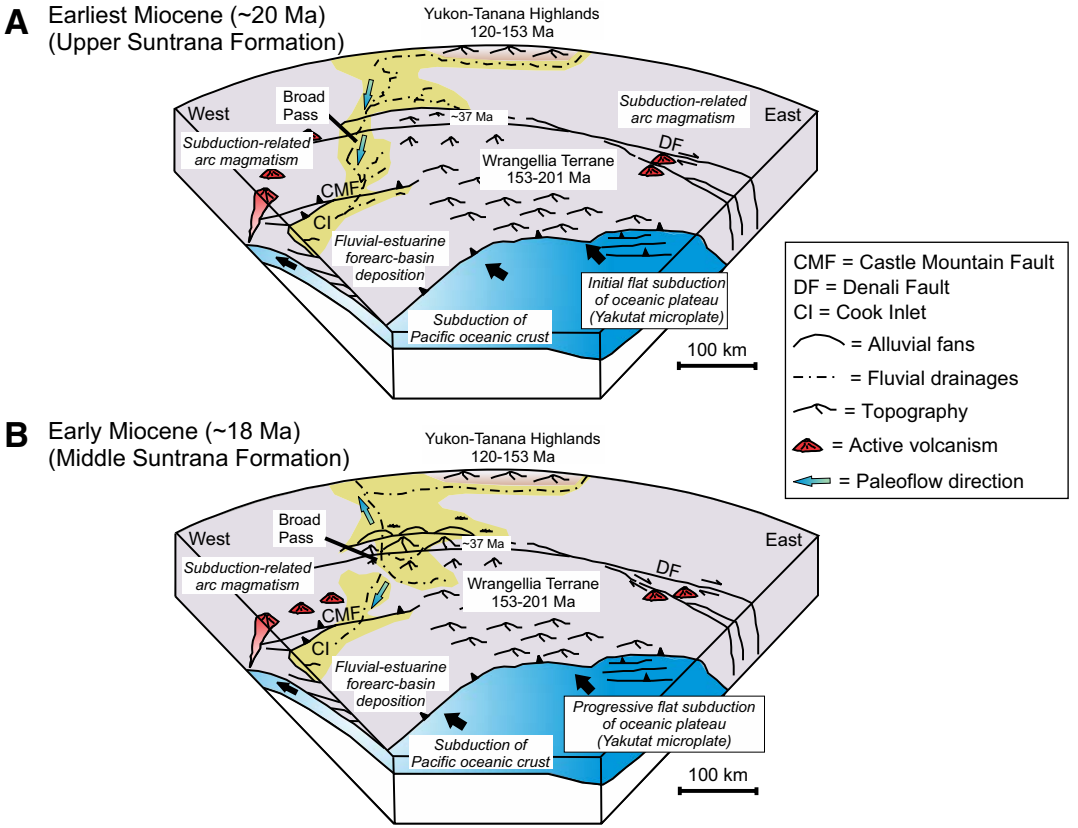

Figure 13. Tectonic diagrams of the Nenana River paleodrainage history during the earliest Miocene (south-flowing) and the early Miocene (north-flowing). Muscovite age populations of unique source regions used for paleoflow constraints are annotated. Figure is modified from Ridgway et al. (2011).

(Fig. 13) also demonstrated that rivers likely crossed the Alaska Range and transported sediment derived from the Yukon-Tanana Highlands into Cook Inlet during pre-Miocene Cenozoic times (Finzel et al., 2016). The same studies make the case that by Miocene time, the Alaska Range was a topographic high affecting sediment routing. These results and interpretations (Finzel et al., 2015, 2016) are in general agreement with the Nenana River ancestral drainage reorganization findings of our study and that of Brennan and Ridgway (2015).

Given the complex nature of strike-slip fault sediment routing systems, where rivers can be sequentially lengthened and captured as water gaps are translated in and out of a drainage's reference frame (Duvall and Tucker, 2015), and given that dominant sediment sources can vary with time as different regions of a transpressive mountain belt can experience focused exhumation with time (Dorsey and Roering, 2006; this study), it is difficult to infer a transpressive river's drainage history from one outcrop location. Putting the documentation of the Tanana Basin change in sediment source—from north of the Alaska Range to south and within the Alaska Range during early Miocene times (Brennan and Ridgway, 2015; this study)—into a broader view of regional Neogene paleodrainage studies of southern Alaska can provide additional insight. Finzel's et al. (2015, 2016) regional findings concluded that sediment in the pre-Miocene Cook Inlet Basin was derived from north of the Alaska Range, and during Miocene times, sediment derived from north of the range ceased to be a source. Additionally, given that the location of the headwaters of the Nenana River system has been generally pinned since ca. 18 Ma (this study), it is reasonable to infer that at least a segment of the upper ancestral Nenana River system experienced a drainage reversal in early Miocene times. Further work is needed to determine the full paleodrainage history of the Nenana River system.

The lag between the initial development of the Alaska Range (ca. 30 Ma to ca. 25 Ma; Benowitz et al., 2014; Lease et al., 2016) and the paleodrainage reversal of the Nenana River system (ca. 18 Ma) deserves further discussion.

Both Benowitz et al. (2011, 2014) and Lease et al. (2016) documented potential asymmetrical topographic development in the Alaska Range. The drainage reorganizational response of transpressive mountain ranges along strike-slip fault systems likely is delayed as topography dynamically varies as crustal blocks are advected through geometric complexities along the strike-slip fault system (e.g., Burkett et al., 2016) and as the overall extent of the range expands (Lease et al., 2016). The process of rivers along strike-slip faults being sequentially lengthened and captured as water gaps are translated into and out of a drainage's reference frame likely also plays a role (Duvall and Tucker, 2015) in the response time between initial increase in surface uplift rates and drainage reversals along transpressive mountain belts.

In summary, during earliest Miocene times, the ancestral Nenana River system flowed to the south into Cook Inlet as the Alaska Range was rising (Fig. 13A), but the Alaska Range was less extensive than today (Bill et al., 2018; Waldien et al., 2018). By the early Miocene (ca. 18 Ma), the upper Nenana River drainage system changed direction from south-directed to north-directed (Fig. 13B). This drainage change was likely due to regional topographic growth exceeding subsidence and/or incision rates in combination with drainage reorganization related to strike-slip translation of water gaps and topographic barriers. By the middle Miocene, the Nenana River drainage system continued to be reorganized as the Alaska Range rose asymmetrically along and across the Denali fault system (Benowitz et al., 2014; Lease et al., 2016). During the latest Miocene and Pliocene, the Healy Creek Formation and lower Suntrana Formation strata to the south of the Suntrana type section locale were likely uplifted, eroded, and recycled into the Tanana Basin. Continued drainage reorganization likely occurred after the inversion of the Tanana Basin at the Suntrana type section location.

Our conclusions do not support a Nenana River reversal at ca. 6 Ma (Wahrhaftig et al., 1969; Ridgway et al., 1999) nor the late Cenozoic timing of an ice stream–driven Nenana River drainage reversal (Moffit, 1915). Our results refine the interpretations of Brennan and Ridgway (2015) in which they inferred there was a change in dominant paleoflow direction from south-directed to north-directed by the time of deposition of the middle Miocene upper Suntrana Formation (ca. 15 Ma; Fig. 13).

The lack of ca. 40 Ma detrital U-Pb zircons in the Usibelli Group and Nenana Gravels (Brennan and Ridgway, 2015) and the presence of ca. 37 Ma $^{40}Ar/^{39}Ar$ detrital muscovite in many of these strata (this study) can be potentially explained by the regional pluton emplacement history during the Eocene in the Alaska Range. The ca. 37 Ma Nenana pluton metamorphic aureole (e.g., muscovite source) was likely unroofed before the deeper but related granitic pluton (e.g., possible zircon source). Hence, $^{40}Ar/^{39}Ar$ analyses of detrital muscovite, a mineral representing potentially shallower crustal levels, provide evidence of a change in unroofing patterns before detrital U-Pb zircon analyses in this case.

In this study, we demonstrated the detrital $^{40}Ar/^{39}Ar$ muscovite geochronology record of paleodrainage reorganization for a long-lived strike-slip fault in a transpressive orogen, reflecting the complex temporal-spatial history of topographic development that is characteristic of these types of mountain ranges. The detrital geochronology signature of paleodrainage reorganization during the development of a continental strike-slip fault transpressive orogen can be expected to vary throughout the life span of the mountain range due in part to (1) the aforementioned complex temporal-spatial topographic history of these mountain ranges and (2) the juxtaposition of diverse source terranes along and across a strike-slip fault–related mountain range.

CONCLUSION

The 17 new bedrock $^{40}Ar/^{39}Ar$ muscovite ages compiled here with 11 published $^{40}Ar/^{39}Ar$ muscovite ages support previous interpretations that the modern period of rapid Alaska Range uplift began by ca. 25 Ma (Benowitz et al., 2014; Lease et al., 2016). This new data set also supports these researchers' interpretations that the focused region of Oligocene to present topographic development in the Alaska Range has varied through time and space due to its nature as a transpressive orogen.

The detrital $^{40}Ar/^{39}Ar$ muscovite signatures of seven Tanana Basin strata (607 single-grain fusion ages) and modern river sediment samples (575 single-grain fusion ages) track the Miocene to present history of paleodrainage reorganization of the Nenana River system. During the deposition of the earliest Miocene (ca. 20 Ma) lower Suntrana Formations, the paleo–Nenana River likely still flowed southward into Cook Inlet, with the Yukon-Tanana Highlands being a dominant source for sediment (Fig. 13A). During the deposition of the early Miocene (ca. 18 Ma) middle Suntrana Formation, sediment sources included significant mica from south of the Alaska Range, possibly from the Wrangellia composite terrane, along with a contribution of sediment unique to the Alaska Range suture zone (Fig. 13B). The middle Miocene upper Suntrana Formation had a large contribution of Triassic-aged muscovite grains, indicating continued drainage reorganization and a likely variable history of rock uplift in the Alaska Range, as also documented through bedrock thermochronology studies (e.g., Benowitz et al., 2014; Lease et al., 2016; this study). During latest Miocene and through Pliocene time, there is evidence of a large population of muscovite grains sourced from the Yukon-Tanana Highlands, implying sediment recycling as the southern extents of the Healy Creek and lower Suntrana Formations were uplifted and eroded. Drainage reorganization likely continued after the deposition of the Pliocene Nenana Gravel unit due in part to slip on the Broad Pass fault or other regional structures.

In conclusion, the Alaska Range was being unroofed by the early Miocene, the Nenana River drainage changed direction by this time period to northward-flowing, and drainage reorganization continued to near modern times driven by tectonic processes. The application of detrital $^{40}Ar/^{39}Ar$ muscovite geochronology to Alaska is a nascent domain but may add further constraints for paleodrainage reconstructions when combined with the more popular detrital U-Pb zircon geochronology approach. We recommend applying both detrital $^{40}Ar/^{39}Ar$ muscovite and U-Pb zircon geochronology to ancient strata and modern river sediment when attempting to reconstruct regional paleodrainage

histories, with the addition of select bedrock dating when regional constraints are lacking. Our overall detrital muscovite work on modern river sediment and ancient strata of the Alaska Range demonstrates that strike-slip fault transpressive orogens can have complex paleodrainage reorganization histories.

ACKNOWLEDGMENTS

This work was partially funded by National Science Foundation (NSF) grant EAR-1249885 to Benowitz and NSF grant EAR-0952834 to Roeske and a University of Alaska Fairbanks Vice Chancellor of Research Office publication grant, and an Undergraduate Research & Scholarly Activity grant to Kailyn Davis. We thank Willis Hames, an anonymous reviewer, and Guest Associate Editor Jamie Jones for constructive and helpful reviews and suggestions that improved the manuscript.

REFERENCES CITED

Annen, C., 2017, Factors affecting the thickness of thermal aureoles: Frontiers of Earth Science, v. 5, p. 82, https://doi.org/10.3389/feart.2017.00082.

Beamud, E., Muñoz, J.A., Fitzgerald, P.G., Baldwin, S.L., Garcés, M., Cabrera, L., and Metcalf, J.R., 2011, Magnetostratigraphy and detrital apatite fission track thermochronology in syntectonic conglomerates: Constraints on the exhumation of the South-Central Pyrenees: Basin Research, v. 23, p. 309–331, https://doi.org/10.1111/j.1365-2117.2010.00492.x.

Beaumont, C., 1981, Foreland basins: Geophysical Journal of the Royal Astronomical Society, v. 65, no. 2, p. 291–329, https://doi.org/10.1111/j.1365-246X.1981.tb02715.x.

Bemis, S.P., and Wallace, W.K., 2007, Neotectonic framework of the north-central Alaska Range foothills, *in* Ridgway, K.D., Trop, J.M., Glen, J.M.G., and O'Neill, J.M., eds., Tectonic Growth of a Collisional Continental Margin: Crustal Evolution of Southern Alaska: Geological Society of America Special Paper 431, p. 549–572, https://doi.org/10.1130/2007.2431(21).

Bemis, S.P., Carver, G.A., and Koehler, R.D., 2012, The Quaternary thrust system of the northern Alaska Range: Geosphere, v. 8, no. 1, p. 196–205, https://doi.org/10.1130/GES00695.1.

Bemis, S.P., Weldon, R.J., and Carver, G.A., 2015, Slip partitioning along a continuously curved fault: Quaternary geologic controls on Denali fault system slip partitioning, growth of the Alaska Range, and the tectonics of south-central Alaska: Lithosphere, v. 7, no. 3, p. 235–246, https://doi.org/10.1130/L352.1.

Benowitz, J.A., Layer, P.W., Armstrong, P., Perry, S.E., Haeussler, P.J., Fitzgerald, P.G., and VanLaningham, S., 2011, Spatial variations in focused exhumation along a continental-scale strike-slip fault: The Denali fault of the eastern Alaska Range: Geosphere, v. 7, no. 2, p. 455–467, https://doi.org/10.1130/GES00589.1.

Benowitz, J.A., Haeussler, P.J., Layer, P.W., O'Sullivan, P.B., Wallace, W.K., and Gillis, R.J., 2012a, Cenozoic tectono-thermal history of the Tordrillo Mountains, Alaska: Paleocene–Eocene ridge subduction, decreasing relief, and late Neogene faulting: Geochemistry Geophysics Geosystems, v. 13, no. 4, Q04009, https://doi.org/10.1029/2011GC003951.

Benowitz, J., Vansant, G., Roeske, S., Layer, P.W., Hults, C.P., and O'Sullivan, P., 2012b, Geochronological constraints on the Eocene to Present slip rate history of the eastern Denali fault system: Geological Society of America Abstracts with Programs, v. 44, no. 7, p. 634.

Benowitz, J.A., Layer, P.W., and Vanlaningham, S., 2014, Persistent long-term (c. 24 Ma) exhumation in the eastern Alaska Range constrained by stacked thermochronology, *in* Jourdan, F., Mark, D.F., and Verati, C., eds., Advances in $^{40}Ar/^{39}Ar$ Dating: From Archaeology to Planetary Sciences: Geological Society, London, Special Publication 378, p. 225–243.

Bill, N.S., Mix, H.T., Clark, P.U., Reilly, S.P., Jensen, B.J., and Benowitz, J.A., 2018, A stable isotope record of late Cenozoic surface uplift of southern Alaska: Earth and Planetary Science Letters, v. 482, p. 300–311, https://doi.org/10.1016/j.epsl.2017.11.029.

Blum, M., and Pecha, M., 2014, Mid-Cretaceous to Paleocene North American drainage reorganization from detrital zircons: Geology, v. 42, no. 7, p. 607–610, https://doi.org/10.1130/G35513.1.

Brennan, P.R., and Ridgway, K.D., 2015, Detrital zircon record of Neogene exhumation of the central Alaska Range: A far-field upper plate response to flat-slab subduction: Geological Society of America Bulletin, v. 127, p. 945–961, https://doi.org/10.1130/B31164.1.

Brocard, G., Teyssier, C., Dunlap, W.J., Authemayou, C., Simon-Labric, T., Cacao-Chiquín, E.N., Gutiérrez-Orrego, A., and Morán-Ical, S., 2011, Reorganization of a deeply incised drainage: Role of deformation, sedimentation and groundwater flow: Basin Research, v. 23, no. 6, p. 631–651, https://doi.org/10.1111/j.1365-2117.2011.00510.x.

Broussard, D., Trop, J.M., Benowitz, J., Daeschler, E.A., Chamberlain, J.A., and Chamberlain, R.B., 2018, Depositional setting, taphonomy and geochronology of new fossil sites in the Catskill Formation (Upper Devonian) of north-central Pennsylvania, USA, including a new early tetrapod fossil: Palaeogeography, Palaeoclimatology, Palaeoecology, v. 511, p. 168–187, https://doi.org/10.1016/j.palaeo.2018.07.033.

Brueseke, M.E., Benowitz, J.A., Trop, J.M., Davis, K.N., Berkelhammer, S.E., Layer, P.W., and Morter, B.K., 2019, The Alaska Wrangell Arc: ~30 million years of subduction-related magmatism along a still active arc-transform junction: Terra Nova, v. 31, p. 59–66, https://doi.org/10.1111/ter.12369.

Burkett, C.A., Bemis, S.P., and Benowitz, J.A., 2016, Along-fault migration of the Mount McKinley restraining bend of the Denali fault defined by late Quaternary fault patterns and seismicity, Denali National Park & Preserve, Alaska: Tectonophysics, v. 693, p. 489–506, https://doi.org/10.1016/j.tecto.2016.05.009.

Cawood, P.A., Hawkesworth, C.J., and Dhuime, B., 2012, Detrital zircon record and tectonic setting: Geology, v. 40, no. 10, p. 875–878, https://doi.org/10.1130/G32945.1.

Chirouze, F., Huyghe, P., Van Der Beek, P., Chauvel, C., Chakraborty, T., Dupont-Nivet, G., and Bernet, M., 2013, Tectonics, exhumation, and drainage evolution of the eastern Himalaya since 13 Ma from detrital geochemistry and thermochronology, Kameng River section, Arunachal Pradesh: Geological Society of America Bulletin, v. 125, no. 3–4, p. 523–538, https://doi.org/10.1130/B30697.1.

Davis, K., Benowitz, J., Layer, P., Trop, J., and Brueseke, M., 2017, Dating the Lost Arc of Alaska: Constraining the timing of the initiation of the Wrangell arc with a new $^{40}Ar/^{39}Ar$ detrital geochronology approach on modern lithic grains: Geological Society of America Abstracts with Programs, v. 49, no. 6, paper no. 107-10, https://doi.org/10.1130/abs/2017AM-296490.

Dodson, M.H., Compston, W., Williams, I.S., and Wilson, J.F., 1988, A search for ancient detrital zircons in Zimbabwean sediments: Journal of the Geological Society [London], v. 145, no. 6, p. 977–983, https://doi.org/10.1144/gsjgs.145.6.0977.

Dorsey, R.J., and Roering, J.J., 2006, Quaternary landscape evolution in the San Jacinto fault zone, Peninsular Ranges of Southern California: Transient response to strike-slip fault initiation: Geomorphology, v. 73, no. 1–2, p. 16–32, https://doi.org/10.1016/j.geomorph.2005.06.013.

Dumoulin, J.A., Jones, J.V., III, Bradley, D.C., Till, A.B., Box, S.E., and O'Sullivan, P., 2018a, Neoproterozoic–early Paleozoic provenance evolution of sedimentary rocks in and adjacent to the Farewell terrane (interior Alaska): Geosphere, v. 14, no. 2, p. 367–394, https://doi.org/10.1130/GES01470.1.

Dumoulin, J.A., Jones, J.V., III, Box, S.E., Bradley, D.C., Ayuso, R.A., and O'Sullivan, P., 2018b, The Mystic subterrane (partly) demystified: New data from the Farewell terrane and adjacent rocks, interior Alaska: Geosphere, v. 14, no. 4, p. 1501–1543, https://doi.org/10.1130/GES01588.1.

Dusel-Bacon, C., Brew, D.A., and Douglass, S.L., 1996, Metamorphic Facies Map of Southeastern Alaska; Distribution, Facies, and Ages of Regionally Metamorphosed Rocks: U.S. Geological Survey Professional Paper 1497-D, 42 p., 2 sheets, scale 1:1,000,000.

Dusel-Bacon, C., Bacon, C.R., O'Sullivan, P.B., and Day, W.C., 2016, Apatite fission-track evidence for regional exhumation in the subtropical Eocene, block faulting, and localized fluid flow in east-central Alaska: Canadian Journal of Earth Sciences, v. 53, no. 3, p. 260–280, https://doi.org/10.1139/cjes-2015-0138.

Dusel-Bacon, C., Holm-Denoma, C.S., Jones, J.V., Aleinikoff, J.N., and Mortensen, J.K., 2017, Detrital zircon geochronology of quartzose metasedimentary rocks from parautochthonous North America, east-central Alaska: Lithosphere, v. 9, no. 6, p. 927–952, https://doi.org/10.1130/L672.1.

Duvall, A.R., and Tucker, G.E., 2015, Dynamic ridges and valleys in a strike-slip environment: Journal of Geophysical Research–Earth Surface, v. 120, no. 10, p. 2016–2026, https://doi.org/10.1002/2015JF003618.

Eberhart-Phillips, D., Christensen, D.H., Brocher, T.M., Hansen, R., Ruppert, N.A., Haeussler, P.J., and Abers, G.A., 2006, Imaging the transition from Aleutian subduction to Yakutat collision in central Alaska, with local earthquakes and active source data: Journal of Geophysical Research–Solid Earth, v. 111, B11303, https://doi.org/10.1029/2005JB004240.

Finzel, E.S., Ridgway, K.D., and Trop, J.M., 2015, Provenance signature of changing plate boundary conditions along a convergent margin: Detrital record of spreading-ridge and flat-slab subduction processes, Cenozoic forearc basins, Alaska: Geosphere, v. 11, no. 3, p. 823–849, https://doi.org/10.1130/GES01029.1.

Finzel, E.S., Enkelmann, E., Falkowski, S., and Hedeen, T., 2016, Long-term fore-arc basin evolution in response to changing subduction styles in southern Alaska: Tectonics, v. 35, no. 7, p. 1735–1759, https://doi.org/10.1002/2016TC004171.

Fitzgerald, P.G., Roeske, S.M., Benowitz, J.A., Riccio, S.J., Perry, S.E., and Armstrong, P.A., 2014, Alternating asymmetric topography of the Alaska range along the strike-slip Denali fault: Strain partitioning and lithospheric control across a terrane suture zone: Tectonics, v. 33, no. 8, p. 1519–1533, https://doi.org/10.1002/2013TC003432.

Garzanti, E., Andò, S., and Vezzoli, G., 2008, Settling equivalence of detrital minerals and grain-size dependence of sediment composition: Earth and Planetary Science Letters, v. 273, p. 138–151, https://doi.org/10.1016/j.epsl.2008.06.020.

Gehrels, G., Rusmore, M., Woodsworth, G., Crawford, M., Andronicos, C., Hollister, L., Patchett, J., Ducea, M., Butler, R., Klepeis, K., and Davidson, C., 2009, U-Th-Pb geochronology of the Coast Mountains batholith in north-coastal British Columbia: Constraints on age and tectonic evolution: Geological Society of America Bulletin, v. 121, no. 9–10, p. 1341–1361, https://doi.org/10.1130/B26404.1.

Greene, A.R., Scoates, J.S., Weis, D., Katvala, E.C., Israel, S., and Nixon, G.T., 2010, The architecture of oceanic plateaus revealed by the volcanic stratigraphy of the accreted Wrangellia oceanic plateau: Geosphere, v. 6, p. 47–73, https://doi.org/10.1130/GES00212.1.

Hacker, B.R., Kelemen, P.B., Rioux, M., McWilliams, M.O., Gans, P.B., Reiners, P.W., Layer, P.W., Söderlund, U., and Vervoort, J.D., 2011, Thermochronology of the Talkeetna intraoceanic arc of Alaska: Ar/Ar, U-Th/He, Sm-Nd, and Lu-Hf dating: Tectonics, v. 30, no. 1, TC1011, https://doi.org/10.1029/2010TC002798.

Haeussler, P.J., Matmon, A., Schwartz, D.P., and Seitz, G.G., 2017a, Neotectonics of interior Alaska and the late Quaternary slip rate along the Denali fault system: Geosphere, v. 13, no. 5, p. 1445–1463, https://doi.org/10.1130/GES01447.1.

Haeussler, P.J., Saltus, R.W., Stanley, R.G., Ruppert, N., Lewis, K., Karl, S.M., and Bender, A., 2017b, The Peters Hills basin, a Neogene wedge-top basin on the Broad Pass thrust fault, south-central Alaska: Geosphere, v. 13, no. 5, p. 1464–1488, https://doi.org/10.1130/GES01487.1.

Hansen, V.L., Heizler, M.T., and Harrison, T.M., 1991, Mesozoic thermal evolution of the Yukon-Tanana composite terrane: New evidence from $^{40}Ar/^{39}Ar$ data: Tectonics, v. 10, no. 1, p. 51–76, https://doi.org/10.1029/90TC01930.

Hodges, K.V., Ruhl, K.W., Wobus, C.W., and Pringle, M.S., 2005, $^{40}Ar/^{39}Ar$ thermochronology of detrital minerals: Reviews in Mineralogy and Geochemistry, v. 58, no. 1, p. 239–257, https://doi.org/10.2138/rmg.2005.58.9.

Hults, C.P., Wilson, F.H., Donelick, R.A., and O'Sullivan, P.B., 2013, Two flysch belts having distinctly different provenance suggest no stratigraphic link between the Wrangellia composite terrane and the paleo-Alaskan margin: Lithosphere, v. 5, no. 6, p. 575–594, https://doi.org/10.1130/L310.1.

Jicha, B.R., Garcia, M.O., and Wessel, P., 2018, Mid-Cenozoic Pacific plate motion change: Implications for the Northwest Hawaiian Ridge and circum-Pacific: Geology, v. 46, no. 11, p. 939–942, https://doi.org/10.1130/G45175.1.

Jones, J., Caine, J., Holm-Denoma, C., Ryan, J., Benowitz, J., and Drenth, B., 2017, Unraveling the boundary between the Yukon-Tanana terrane and the parautochthonous North America in eastern Alaska: Geological Society of America Abstracts with Programs, v. 49, no. 6, paper no. 148-9, https://doi.org/10.1130/abs/2017AM-304142.

Lawrence, R.L., Cox, R., Mapes, R.W., and Coleman, D.S., 2011, Hydrodynamic fractionation of zircon age populations: Geological Society of America Bulletin, v. 123, no. 1–2, p. 295–305, https://doi.org/10.1130/B30151.1.

Lease, R.O., Haeussler, P.J., and O'Sullivan, P., 2016, Changing exhumation patterns during Cenozoic growth and glaciation of the Alaska Range: Insights from detrital thermochronology and geochronology: Tectonics, v. 35, no. 4, p. 934–955, https://doi.org/10.1002/2015TC004067.

Leopold, E.B., and Liu, G., 1994, A long pollen sequence of Neogene age, Alaska Range: Quaternary International, v. 22–23, p. 103–140, https://doi.org/10.1016/1040-6182(94)90009-4.

Martin, A.J., Copeland, P., and Benowitz, J.A., 2015, Muscovite $^{40}Ar/^{39}Ar$ ages help reveal the Neogene tectonic evolution of the southern Annapurna Range, central Nepal, *in* Mukherjee, S., Carosi, R., van der Beek, P.A., Mukherjee, B.K., and Robinson, D.M., eds., Tectonics of the Himalaya: Geological Society, London, Special Publication 412, p. 199–220.

McDougall, I., and Harrison, T.M., 1999, Geochronology and Thermochronology by the $^{40}Ar/^{39}Ar$ Method (2nd ed.): New York, Oxford University Press, 269 p.

Moffit, F.H., 1915, The Broad Pass region, Alaska: U.S. Geological Survey Bulletin 608, 80 p., 2 sheets, scale 1:250,000.

Nokleberg, W.J., Jones, D.L., and Silberling, N.J., 1985, Origin and tectonic evolution of the Maclaren and Wrangellia terranes, eastern Alaska Range, Alaska: Geological Society of America Bulletin, v. 96, no. 10, p. 1251–1270, https://doi.org/10.1130/0016-7606(1985)96<1251:OATEOT>2.0.CO;2.

Nokleberg, W.J., Aleinikoff, J.N., Dutro, J.T., Jr., Lanphere, M.A., Silberling, N.J., Silva, S.R., Smith, T.E., and Turner, D.L., 1992, Map, Tables, and Summary of Fossil and Isotopic Age Data, Mount Hayes Quadrangle, Eastern Alaska Range, Alaska: U.S. Geological Survey Miscellaneous Field Studies Map 1996-D, 43 p., 1 sheet, scale 1:250,000.

Perry, S.E., 2014, Thermotectonic Evolution of the Alaska Range: Low-Temperature Thermochronologic Constraints [Ph.D. dissertation]: Syracuse, New York, Syracuse University, 844 p.

Perry, S.E., Fitzgerald, P.G., and Benowitz, J.A., 2010, Thermotectonic evolution of the eastern Alaska Range: Constraints from low-temperature thermochronology, *in* Proceedings of the 12th International Conference on Thermochronology, 16–20 August 2010, Glasgow, Scotland, p. 268.

Riccio, S.J., Fitzgerald, P.G., Benowitz, J.A., and Roeske, S.M., 2014, The role of thrust faulting in the formation of the eastern Alaska Range: Thermochronological constraints from the Susitna Glacier thrust fault region of the intracontinental strike-slip Denali fault system: Tectonics, v. 33, no. 11, p. 2195–2217, https://doi.org/10.1002/2014TC003646.

Ridgway, K.D., Trop, J.M., and Sweet, A.R., 1997, Thrust-top basin formation along a suture zone, Cantwell basin, Alaska Range: Implications for development of the Denali fault system: Geological Society of America Bulletin, v. 109, no. 5, p. 505–523, https://doi.org/10.1130/0016-7606(1997)109<0505:TTBFAA>2.3.CO;2.

Ridgway, K.D., Trop, J.M., and Jones, D.E., 1999, Petrology and provenance of the Neogene Usibelli Group and Nenana Gravel: Implications for the denudation history of the central Alaska Range: Journal of Sedimentary Research, v. 69, no. 6, p. 1262–1275, https://doi.org/10.2110/jsr.69.1262.

Ridgway, K.D., Trop, J.M., Nokleberg, W.J., Davidson, C.M., and Eastham, K.R., 2002, Mesozoic and Cenozoic tectonics of the eastern and central Alaska Range: Progressive basin development and deformation in a suture zone: Geological Society of America Bulletin, v. 114, no. 12, p. 1480–1504, https://doi.org/10.1130/0016-7606(2002)114<1480:MACTOT>2.0.CO;2.

Ridgway, K.D., Thoms, E.E., Layer, P.W., Lesh, M.E., White, J.M., and Smith, S.V., 2007, Neogene transpressional foreland basin development on the north side of the central Alaska Range, Usibelli Group and Nenana Gravel, Tanana Basin, *in* Ridgway, K.D., Trop, J.M., Glen, J.M.G., and O'Neill, J.M., eds., Tectonic Growth of a Collisional Continental Margin: Crustal Evolution of Southern Alaska: Geological Society of America Special Paper 431, p. 507–547, https://doi.org/10.1130/2007.2431(20).

Ridgway, K.D., Trop, J.M. and Finzel, E.S., 2011, Modification of continental forearc basins by flat-slab subduction processes: A case study from southern Alaska: Tectonics of Sedimentary Basins: Recent Advances, p. 327–346, https://doi.org/10.1002/9781444347166.ch16.

Roeske, S., Benowitz, J., and O'Sullivan, P.B., 2012, Late Eocene syntectonic magmatism along the dextral Denali fault provides constraints on timing of strike-slip displacement: San Francisco, California, American Geophysical Union, Fall Meeting supplement, abstract T11A–2548.

Salazar-Jaramillo, S., Fowell, S.J., McCarthy, P.J., Benowitz, J.A., Śliwiński, M.G., and Tomsich, C.S., 2016, Terrestrial isotopic evidence for a middle-Maastrichtian warming event from the lower Cantwell Formation, Alaska: Palaeogeography, Palaeoclimatology, Palaeoecology, v. 441, p. 360–376, https://doi.org/10.1016/j.palaeo.2015.09.044.

Sharman, G.R., Covault, J.A., Stockli, D.F., Wroblewski, A.F.J., and Bush, M.A., 2017, Early Cenozoic drainage reorganization of the United States Western Interior–Gulf of Mexico sediment routing system: Geology, v. 45, p. 187–190, https://doi.org/10.1130/G38765.1.

Smith, N.D., 1972, Some sedimentological aspects of planar cross-stratification in a sandy braided river: Journal of Sedimentary Research, v. 42, no. 3, p. 624–634.

Spotila, J.A., House, M.A., Niemi, N.A., Brady, R.C., Oskin, M., Buscher, J.T., Till, A.B., Roeske, S.M., Sample, J.C., and Foster, D.A., 2007, Patterns of bedrock uplift along the San Andreas fault and implications for mechanisms of transpression, *in* Till, A.B., Roeske, S.M., Sample, J.C., and Foster, D.A., eds., Exhumation Associated with Continental Strike-Slip Fault Systems: Geological Society of America Special Paper 434, p. 15–33, https://doi.org/10.1130/2007.2434(02).

Staples, R.D., Gibson, H.D., Colpron, M., and Ryan, J.J., 2016, An orogenic wedge model for diachronous deformation, metamorphism, and exhumation in the hinterland of the northern Canadian Cordillera: Lithosphere, v. 8, no. 2, p. 165–184, https://doi.org/10.1130/L472.1.

Terhune, P., Benowitz, J., Trop, J., and O'Sullivan, P., 2017, Thermochronology of the Talkeetna Mountains of southern Alaska: Cenozoic topographic development history: Geological Society of America Abstracts with Programs, v. 49, no. 6, paper no. 214-8.

Thoms, E.E., 2000, Late Cenozoic Unroofing Sequence and Foreland Basin Development of the Central Alaska Range: Implications from the Nenana Gravel [M.S. thesis]: Fairbanks, Alaska, University of Alaska–Fairbanks, 215 p.

Tomsich, C.S., McCarthy, P.J., Fiorillo, A.R., Stone, D.B., Benowitz, J.A., and O'Sullivan, P.B., 2014, New zircon U-Pb ages for the lower Cantwell Formation: Implications for the Late Cretaceous

paleoecology and paleoenvironment of the lower Cantwell Formation near Sable Mountain, Denali National Park and Preserve, central Alaska Range, USA, *in* Stone, D.B., Grikurov, E.G., Clough, J.G., Oakey, G.N., and Thurston, D.K., eds., ICAM VI: Proceedings of the International Conference on Arctic Margins VI: Fairbanks, Alaska, p. 19–60.

Triplehorn, D.M., Drake, J., and Layer, P.W., 2000, Preliminary $^{40}Ar/^{39}Ar$ ages from two units in the Usibelli Group, Healy, Alaska: New light on some old problems, *in* Pinney, D.S., and Davis, P.K., eds., Short Notes on Alaska Geology 1999: Alaska Division Geological and Geophysical Surveys Professional Report 119, p. 117–127, https://doi.org/10.14509/2682.

Trop, J.M., and Ridgway, K.D., 2007, Mesozoic and Cenozoic tectonic growth of southern Alaska: A sedimentary basin perspective, *in* Ridgway, K.D., Trop, J.M., Glen, J.M.G., and O'Neill, J.M., eds., Tectonic Growth of a Collisional Continental Margin: Crustal Evolution of Southern Alaska: Geological Society of America Special Paper 431, p. 55–94, https://doi.org/10.1130/2007.2431(04).

van Hoang, L., Wu, F.Y., Clift, P.D., Wysocka, A., and Swierczewska, A., 2009, Evaluating the evolution of the Red River system based on in situ U-Pb dating and Hf isotope analysis of zircons: Geochemistry Geophysics Geosystems, v. 10, Q11008, https://doi.org/10.1029/2009GC002819.

van Hoang, L., Clift, P.D., Mark, D., Zheng, H., and Tan, M.T., 2010, Ar-Ar muscovite dating as a constraint on sediment provenance and erosion processes in the Red and Yangtze River systems, SE Asia: Earth and Planetary Science Letters, v. 295, p. 379–389, https://doi.org/10.1016/j.epsl.2010.04.012.

Vermeesch, P., 2004, How many grains are needed for a provenance study?: Earth and Planetary Science Letters, v. 224, p. 441–451, https://doi.org/10.1016/j.epsl.2004.05.037.

Wahrhaftig, C., 1987, The Cenozoic section at Suntrana Creek, Alaska, *in* Hill, M.L., ed., Cordilleran Section of the Geological Society of America: Centennial Field Guide Volume 1: Boulder, Colorado, Geological Society of America, p. 445–450.

Wahrhaftig, C., Wolfe, J.A., Leopold, E.B., and Lanphere, M.A., 1969, The Coal-Bearing Group in the Nenana Coal Field, Alaska: U.S. Geological Survey Bulletin 1274-D, 30 p.

Waldien, T., Roeske, S., Benowitz, J., Allen, W.K., and Ridgway, K., 2015, Neogene exhumation in the eastern Alaska Range and its relationship to splay fault activity in the Denali fault system: San Francisco, California, American Geophysical Union, Fall Meeting supplement, abstract T42B-02.

Waldien, T.S., Roeske, S.M., Benowitz, J.A., Allen, W.K., Ridgway, K.D., and O'Sullivan, P.B., 2018, Late Miocene to Quaternary evolution of the McCallum Creek thrust system, Alaska: Insights for range-boundary thrusts in transpressional orogens: Geosphere, v. 6, p. 2379–2406, https://doi.org/10.1130/GES01676.1.

Wiedmer, M., Montgomery, D.R., Gillespie, A.R., and Greenberg, H., 2010, Late Quaternary megafloods from Glacial Lake Atna, southcentral Alaska, USA: Quaternary Research, v. 73, p. 413–424, https://doi.org/10.1016/j.yqres.2010.02.005.

Wilson, F.H., Hults, C.P., Mull, C.G. and Karl, S.M., 2015, Geologic Map of Alaska: U.S. Geological Survey Scientific Investigations Map 3340, 197 p., 2 sheets, scale 1:1,584,000.

Zhang, T., and Sun, H., 2011, Phylogeographic structure of *Terminalia franchetii* (Combretaceae) in southwest China and its implications for drainage geological history: Journal of Plant Research, v. 124, no. 1, p. 63–73, https://doi.org/10.1007/s10265-010-0360-3.